Characterising the origin, nature and fate of sediment exported from catchments perturbed by active tectonics

Citation for published version:
Whittaker, AC, Attal, M & Allen, PA 2010, 'Characterising the origin, nature and fate of sediment exported from catchments perturbed by active tectonics', *Basin Research*, vol. 22, no. 6, pp. 809-828.
https://doi.org/10.1111/j.1365-2117.2009.00447.x

Digital Object Identifier (DOI):
10.1111/j.1365-2117.2009.00447.x

Link:
Link to publication record in Edinburgh Research Explorer

Document Version:
Peer reviewed version

Published In:
Basin Research

Cite As: Whittaker, AC, Allen, PA & Attal, M 2010, 'Characterising the origin, nature and fate of sediment exported from catchments perturbed by active tectonics' *Basin Research*, vol 22, no. 6, pp. 809-828.

DOI: 10.1111/j.1365-2117.2009.00447.x

Characterising the origin, nature and fate of sediment exported from catchments perturbed by active tectonics

Authors: Alexander C. Whittaker, Mikael Attal, Philip A. Allen

Address for correspondence:

Alexander C. Whittaker
Department of Earth Science and Engineering,
Royal School of Mines
Imperial College
London SW7 2AZ

a.whittaker@imperial.ac.uk

Characterising the origin, nature and fate of sediment exported from catchments perturbed by active tectonics.

Alexander C. Whittaker[1†], Mikaël Attal[2] and Philip A. Allen[1]

[1]Department of Earth Science and Engineering, Royal School of Mines, Imperial College, London, SW7 2AZ, UK

[2]School of GeoSciences, University of Edinburgh, Drummond Street, Edinburgh, EH8 9XP

Key words:

faults, sediment, tectonics, landslides, upland catchments, transient landscape, basin stratigraphy

[†]**corresponding author**

tel: (+44) 79309 57816

a.whittaker@imperial.ac.uk

ABSTRACT

Changes to the tectonic boundary conditions governing erosional dynamics in upland catchments have a significant effect on the nature and magnitude of sediment supply to neighbouring basins. While these links have been explored in detail by numerical models of landscape evolution, there has been relatively little work to quantify the timing, characteristics and locus of sediment release from upland catchments in response to changing tectonic boundary conditions that are well-constrained independently. We address this challenge by quantifying the volume and granulometric characteristics of sediment exported from modern rivers draining across active normal faults in the Central Apennines in Italy. We demonstrate that catchments undergoing a transient response to tectonics are associated with significant volumetric export of material derived solely from the zone upstream of the fault, producing bi-modal grain-size distributions with elevated D_{84} values within the transient reach. This is in direct contrast to the headwaters, where the fluvial capacity to transport sediment is low and the grain-size distribution of material in transit is fine and uni-modal. This response is driven by input from coupled hillslopes, and we show the amplitude of the signal is modulated by the degree of tectonic perturbation, once the threshold for bedrock landsliding is exceeded. Additionally, we evaluate the length-scale over which this transient grain-size signal propagates downstream into the basin. We show that the coarse-fraction sediment released is likely to be retained in the proximal hanging-wall if rates of tectonic subsidence are high and if the axial river system is small or far from the fault-bounded mountain front. Our results challenge the view that sediment is sourced uniformly from tectonically-active catchments and demonstrate that transient responses control the locus, magnitude and calibre of sediment supply to basins.

1. Introduction

1.1 Rationale

Where does sediment come from? The question is a simple one, but it is central to any treatment of the Earth's surface as an integrative process system that explicitly links sediment production and export to far-field deposition (*Leeder et al., 1998; Castelltort & Van den Driessche, 2003; Dadson et al., 2003; Stock et al., 2006; Allen, 2008*). In a generic sense, it has been long established that much of the sediment that ends up in depositional basins is initially sourced from or via fluvial erosion in upland catchments, and that this erosional engine is driven primarily by the interaction of tectonics and climate (e.g. *Milliman & Syvitski, 1992, Talling & Sowter, 1998; Burbank & Pinter, 1999; Whipple, 2004; Allen, 2007*). Moreover, we know that sedimentary basins represent one of the most significant archives to document the evolution of Earth's environments through time (*Tucker & Slingerland, 1996*; *Hovius & Leeder, 1998*; *Gawthorpe & Leeder, 2000*; *Allen & Allen, 2005*). These statements have two important implications: Firstly, that tectono-climatically influenced changes in sediment supply (whether bulk volume, composition, or grain-size) exert a first order control on the locus and nature of sediment facies found in these basins (e.g. *Tucker & Slingerland, 1998; Paola & Swenson, 1998; Molnar, 2001*). Secondly, that he stratigraphic record of deposition can be inverted, at least in principle, to say something about the changing controls on sediment production through time as function of these boundary conditions (*Robinson & Slingerland, 1998*; *Densmore et al., 2007*).

More recently, controls on the distribution and locus of erosion have become a fundamental concern for quantitative geomorphologists seeking to understand the dynamic behaviour of the earth's surface. Sediment removal not only shapes the landscape, but dynamically controls the rates and process of fluvial incision into bedrock, enhancing downcutting if the relative supply rate is low, but reducing it when sediment supply approaches the theoretical transport capacity of the flow (*Sklar & Dietrich, 2004*). Significantly, *Cowie et al.* (*2008*) demonstrate explicitly that this effect controls the tempo and style of landscape evolution on timescales approaching 10^6 years, and therefore, the magnitude and characteristics of erosional fluxes from upland catchments.

These studies underline the fact that understanding the controls on sediment release from catchments remains a key challenge for both sedimentary geologists seeking to couple sediment production with transport and deposition downstream, and geomorphologists looking to improve our understanding of landscape dynamics. To make progress in this area, we therefore need to link the growing insight into the geomorphic response of catchments to boundary condition change (e.g. *Whipple & Tucker, 2002; Cowie et al, 2006; Whittaker et al., 2007a*) with existing sedimentological data of where and when material is actually deposited in basins (e.g. *Horton et al., 2004*). Unfortunately, our ability to do this is hindered in two main ways: Firstly, because we presently have poor field constraints (as opposed to numerical model predictions) how, when and where sediment is sourced from upland catchments in response to external perturbation over geologically relevant time periods (i.e. $>10^6$ years), and secondly because few studies have successfully linked detailed information from young depositional stratigraphy to the sediment characteristics of the actively eroded upland source area (c.f. *Allen & Densmore, 2000*; *Allen, 2008*).

This paper bridges this key research problem. We quantifying the magnitude and nature of sediment fluxed from fluvial catchments in the Central Apennines in Italy that are bounded downstream by normal faults whose tectonic and geomorphic evolution are already well-understood (*Roberts & Michetti*, 2004; *Whittaker et al.*, 2007b). We contrast the grain-size distribution of sediment exported from catchments in topographic steady state (i.e. catchments where erosion matches uplift at any point) with catchments that are undergoing a transient response to a change in fault slip rate which has taken place within the last 1 My (c.f. *Whittaker al., 2007b*). We then evaluate how this grain-size signal evolves downstream and we compare this data-set with Pliocene-Recent sediments preserved in the normal fault bounded Fucino basin, where the hanging-wall stratigraphy is well-characterised. Our results invalidate the assumption that sediment is sourced uniformly from tectonically active catchments and demonstrate that transient responses to changes in fault slip rate can control the locus, magnitude and calibre of sediment supply to, and deposition within fault-bounded basins. More widely, we offer new insights for geomorphologists seeking to decode the interactions between hillslopes, sediment flux and channel incision in transient landscapes, and we provide a fresh perspective for sedimentologists trying to predict proximal hanging-wall stratigraphy in normal fault bounded terrains.

1.2 Background and Existing Work

The concept of the Earth's surface as forming a sediment routing system that transfers mass from source to sink has gained considerable traction in recent years (*Hovius & Leeder, 1998*; *Castelltort & Van den Driessche, 2003; Allen, 2008*). Such conceptual models emphasise the important role of sediment supply characteristics, often couched in terms of probability density function (*pdf*) of grain-size, volume or composition, in determining the characteristics of depositional stratigraphy (e.g. *Paola & Swenson, 1998*). Sediment *pdfs* vary as function of external boundary conditions such as lithology or tectonics, and are modified by fluvial processes during subsequent transport (e.g. *Attal & Lavé*, 2006). Existing field studies have demonstrated how these bulk supply characteristics interact with tectonics interact to determine depositional stratigraphy (e.g. *Heller & Paola, 1992, Elliet & Gawthorpe, 1995; Gawthorpe & Leeder, 2000*). However, many studies that attempt to invert the stratigraphic record from the "downstream" perspective (sensu *Hovius & Leeder, 1998)* tend to focus on the dominant control of tectonic subsidence in generating accommodation space and determining stratal architecture (*Fedele & Paola, 2007)* or are content to model bulk sediment volumes or 'average' grain-sizes being produced from supposedly spatially uniform erosion upstream (e.g. *Robinson & Slingerland, 1998; Weltje et al., 1998; Schlunegger, 2002; Horton et al., 2004*). These studies therefore reduce the complexity of sediment supply in catchments to that of a fixed upstream point source.

In conjunction with the above work, "upstream" insight into the dynamics of catchment-wise sediment export in recent years has been generated as a product of burgeoning growth in landscape science in the last 10 years (*Hardy & Gawthorpe, 2002*, *Whipple, 2004; Cowie et al., 2006*). A growing number of field studies (e.g. *Montgomery & Stolar, 2006; Whittaker et al. 2007a; Cowie et al., 2008*) and a considerable body of modelling work (e.g. *Tucker & Slingerland, 1996; Allen & Densmore, 2000; Whipple & Tucker, 1999; Willett & Brandon, 2002; Tucker & Whipple, 2002; Hardy & Gawthorpe, 2002; Simpson, 2006*) have evidenced the coupling between tectonics, climate, and erosion through time, and demonstrate that transient landscape response to both tectonic and climatic perturbations can be associated with significant changes in the flux of sediment from upland areas. Recent work by Densmore et al., (*2007*) for small fans using a mass balance approach explicitly shows for transport-limited (i.e. diffusive) catchments how the amplitude and timescale of sediment flux to basins is controlled by changes in fault slip rate, and demonstrates this has significant implications for hangingwall stratigraphy in cases where the sediment budget is closed. However, such models do not typically give explicit information about the calibre of sediment exported. Additionally, upland catchments do not necessarily respond, for example to changes in tectonic uplift rate, by purely diffusive means. This is particularly true for under-supplied bedrock rivers (e.g. detachment-limited river systems) where the transient response to a change in tectonic uplift rate has been associated with a "wave" of incision that migrates up the catchment as the landscape attempts to reach a new topographic steady-state over timescales > 1 My (*Whipple & Tucker, 2002*; *Whittaker et al., 2007a, Whittaker et al., 2007b*). Moreover, research in the last ten years also points to the coupling of hill-slopes and channel systems as being crucial to the transmission of this tectonic signal to the whole landscape over timescales of 10^4-10^6 years (*Roering et al., 1999; Roering et al., 2001; Whittaker et al., 2007a; Mudd & Furbish., 2007*). Incision-driven landsliding is therefore responsible for supplying considerable volumes of sediment directly to axial channels (e.g. *Hovius et al.*, 2000; *Lavé & Burbank*, 2004; *Attal & Lavé, 2006; Ouimet et al., 2007*). Unfortunately, field studies that document this supply signal often focus on short term (i.e. < 10^2 years) monitoring (*Schlunneger et al., 2002; Casagli et al., 2003; Schuerch et al., 2006*) and are not typically contextualised either with respect to their downstream impact on fluvial sediment characteristics, or to the longer term tectonic or climatic boundary conditions governing the landscape. Consequently there has been little work on the nature and characteristics of sediment liberated during the process of adjustment to the new boundary conditions.

In this study we take advantage of a unique study area in the Central Apennines (section 2)) to investigate the dynamics and key controls on sediment export from upland catchments perturbed by active tectonics. Our approach is to document the quantity and nature of material in transport from modern day catchments draining across active normal faults that differ in terms of their history and magnitude of slip (section 4). We then compare this with (i) the locus and calibre of sediment supplied both from upstream and from hill-slope sources and (ii) preserved stratigraphy downstream (section 5). In particular, the results allow us to explore the impact of transient responses to tectonics on sediment supply to basins.

2. Regional Setting

The Central Apennines of Italy are a NE verging imbricate fold and thrust belt that formed as a result of convergence between the Eurasian and African plates (*D'Agostino & Jackson, 2001; Roberts & Michetti, 2004*). While thrusting continues today on the Adriatic margin of the mountain chain (*Patacca et al., 1990; Pizzi, 2003; Centamore & Nisio, 2003*) a zone of extension has formed behind the compressional front since the late Pliocene (ca. ~ 3 Ma) (Fig. 1a) apparently driven by roll-back of the Calabrian subduction zone (*Lavecchia et al, 1994, D'Agostino et al, 2001*). As a result, a network of SE-NW striking normal faults has developed that accommodates stretching of approximately 6 mm/yr across this part of Italy (*Hundstat et al., 2003*; *Roberts & Michetti, 2004*). These faults are also uplifted on a long-wavelength topographic bulge that is supported dynamically by mantle convection (*D'Agostino & McKenzie, 1999*), with many basins having minimum elevations > 500 m. The normal faults uplift Mesozoic platform carbonates, while the associated hanging-wall basins (*Accordi et al., 1986*) are filled by fluvial and lacustrine continental deposits from the Late Pliocene to Recent (Fig. 1b), and hence considered contemporaneous with extension (*Cavinato, 1993; Cavinato & DeCelles, 1999; Cavinato et al, 2002*). Some of these hanging-wall basins remain internally-drained, and thus preserve the full stratigraphy from 3 Ma to present (e.g. Fucino basin, Fig. 1c).

Significantly, the normal fault array is one the best constrained in the world in terms of the variation in both displacement and slip rate along each of the fault strands; rates of throw have been calculated for a variety of time periods using methods as diverse as integrated seismic and borehole surveys (*Cavinato et al., 2002*), measurements of fault scarp offsets (*Morewood & Roberts*, 2002) and cosmogenic dating of fault scarps (*Palumbo et al., 2004*). A full review can be found in *Roberts &*

Michetti, (2004). Throw and throw rate vary across the array, with the largest values (throw ~ 2 km; throw rate ~2 mm/yr) for the Fucino fault, near the centre of the array (Fig. 1c). Slip rates < 0.4mm/yr are documented for faults at the north and south edges of the array (e.g. Leonessa and S. Cassino faults), and distally located faults on the far west of the Apennines show no Holocene displacement at all. Moreover, slip rates on some of the faults have varied through time as a result of fault growth and interaction (*Cowie & Roberts, 2001; Roberts & Michetti, 2004; Whittaker et al., 2008*). Faults which are known to have undergone such a slip rate increase are highlighted in Fig. 1b. A synthesis of geological mapping, seismic survey results and numerical modelling suggests that this fault-interaction driven slip-rate increase occurred at ~0.8 Ma for the centrally located faults (*Cowie & Roberts, 2001*), while distal faults have moved at a constant rate for 3 My (*Roberts & Michetti, 2004*).

Importantly, recent work in the area (*Whittaker et al., 2007a, b, 2008*) has shown that catchments draining across increased slip-rate normal faults are still undergoing a transient response to this tectonic perturbation. This transient landscape response is associated with the formation of convex reaches and gorges in the rivers upstream of the fault, narrowed channel and valley in this zone, rejuvenated hill-slopes and the migration of the drainage divide towards the fault (see *Whittaker et al., 2007b* for a full review). In contrast, rivers that cut across faults which have moved at a constant rate for the past 3 My appear to have reached topographic steady-state and do not display these transient characteristics (*Whittaker et al., 2007b*). Because transient landscape responses should theoretically have a substantial impact on the rates and characteristics of sediment export from catchments (section 1.2; *Whipple & Tucker, 2002; Cowie et al., 2006*), the Central Apennines is an excellent natural laboratory to study the control of tectonics on sediment production, transport and deposition in normal fault bounded terrains..

3. Methodology

We quantify the volume and characteristics of sediment exported from five catchments in the Central Apennines known to be undergoing a transient response to tectonics (*Whittaker et al., 2008*) and compare this with two rivers which are crossing active normal faults, but which have reached topographic steady-state (*Whittaker et al., 2007b*). The rivers are (Fig. 1c):

i) The Rio Torto, which crosses the Fiamignano fault at a point where the present day throw rate is 1 mm/yr; its catchment drainage area, (*A*) is 62 km^2.

ii) The Torrente L'Apa, which crosses the Fiamignano fault at a point where the present day throw rate is ~0.25 mm/yr; *A* = 25 km^2.

iii) The Celano Gorge, which crosses the Fucino fault where the present day throw rate is 1.5 mm/yr; *A* = 41 km^2.

iv) The Rio di Aielli, which also crosses the Fucino fault where the present day throw rate is ~1.5 mm/yr; *A* = 31 km^2.

v) La Canala, which crosses the Pescasseroli fault where the present day throw rate is 0.5mm/yr; *A* = 18 km^2.

All these faults (red lines, Fig. 1c) underwent a slip-rate increase at 0.8 Ma (*Cowie & Roberts, 2001*) and for all the channels except the Torrente L'Apa, the maximum slip-rate prior to the fault array becoming soft-linked was ~0.3 mm/yr (*Roberts & Michetti, 2004*). For the Torrente L'Apa, the slip rate prior to throw rate increase was < 0.1 mm/yr (*Whittaker et al., 2008*). Each of these catchments has a pronounced convexity (knickzone) in the long profile of the trunk stream, upstream of the active fault (Fig. 2; see also *Whittaker et al., 2008*). The break in slope in these long profiles, upstream of the fault, represents the length scale over which the river has managed to increase its incision rate to match the fault uplift rate since 0.8 Ma (*Whittaker et al., 2007b; Attal et al., 2008*), and consequently where the hill-slopes have been rejuvenated. Upstream of the break in slope, the catchments have not yet detected the change in the tectonic uplift rate. Consequently the stretch of river upstream of the fault and downstream of the break in slope represents the zone where the "additional" incision related to the increase in fault slip rate is located.

We compare these drainages to the following two river systems that cross constant slip-rate faults (black lines, Fig. 1c) and have reached topographic steady-state (*Whittaker et al., 2007b*):

vi) the Fosso Tascino, draining an uplifted horst between the Rieti and Leonessa faults, and which crosses the latter structure where the present day throw rate is 0.3 mm/yr; A = 45 km^2.

vii) The Valleluce River, which crosses the South Cassino fault where the present throw rate is 0.25-0.3 mm/yr; A = 20 km^2.

These rivers have concave-up longitudinal profiles (concavity = 0.59, 0.51 respectively, (Fig. 2; *Whittaker et al., 2008*)), and the distribution of unit stream power downstream matches the distribution of uplift in the footwall of the fault (*Whittaker et al., 2007b*).

We make a first order estimate of the total additional volume of sediment released from catchments undergoing a transient response to tectonics by projecting the concave long profile of the channel above the break in slope in Fig. 2 to the fault, and calculating the total volume of catchment beneath this (the incised zone). We also quantify the present day grain-size of bed-load exported from these catchments by measuring, at regular intervals (i.e. every 200-500m) downstream, the sediment calibre of material in gravel bars mobilised during high flow events. Note that while these catchments are strongly undersupplied, with significant exposures of bedrock along the channel, sediment covers some of bed in a number of localities (*Whittaker et al., 2007b; Whittaker et al., 2008; Cowie et al., 2008*). For most of the catchments, we characterise the sediment calibre by using the Wolman point count method (*Wolman, 1954*): the major and minor axes of 100-300 individual randomly-selected clasts > 1 mm in diameter are measured in order to estimate the median grain-size value, D_{50}, and the 84th percentile, D_{84}, of the deposits. Additionally, our ancillary observations show that D_{50} estimates fluctuate by < ±0.5 mm with increasing number of measurements in excess of 100 grains, suggesting that this method produces robust data. This approach has the significant advantages of widespread use and ease and rapidity of execution, while yielding more easily reproducible results than other methods of sampling such as zig-zag sampling downstream (*Kondolf, 1997*).

However, for the Rio Torto, and the Celano gorge which are both undergoing a significant transient response to tectonic perturbation because they have experienced relative throw rate increases of 3 and 5 times respectively, we have also compiled a full weighted grain-size distribution of the coarse fraction (≥ 1cm) of bedload for downstream sample points. We typically sieved between 40 and 100 kg of sediment at each locality, using a hand-held weighing scale with a nominal precision of 10 g. Sieve sizes were scaled at 1-2, 2-4, and 4-8 cm respectively. The surface layer of sediment was removed, so that results were not affected by winnowing, which could preferentially coarsen the surface of gravel bars (c.f. *Attal & Lavé, 2006*). Cobbles with two principle axes longer than 8 cm were individually weighed and a representative diameter was calculated, assuming that the particle was spherical and had a density of 2400 kg/m^3. D_{50} and D_{84} could then be accurately determined from cumulative frequency graphs of fractional weight proportion as a function of increasing grain-size. Following Kellerhals & Bray (*1971*), we tried to ensure that the largest clast was < 10% of the total weight of the sample so as to reduce bias in our estimates of the coarse sediment D_{84} value.

Because channels undergoing a transient response to tectonics typically couple to the adjacent hill-slopes (c.f. *Mudd & Furbish, 2007; Ouimet et al., 2007*), we also documented the position of landslide deposits larger than ~ 100 m^3 that were supplying material to the channels. For the Rio Torto, which is the best characterised of these channels in terms of the geometric adjustment of the channel to the tectonic perturbation (see *Whittaker et al., 2007a; Whittaker et al., 2008*), we also quantified the grain-size distribution of typical landslides and scree cones which were supplying material directly to the channel, using the weighted grain-size distribution methodology described above.

Finally for the Celano Gorge and Rio di Aielli, where there are good exposures of the basin fill uplifted on small fault splays and excellent stratigraphic constraints on the evolution of hanging-wall sedimentation from seismic lines (Cavinato et al., 2002; Whittaker et al., 2008), we also evaluated the calibre of material preserved in exposed upper Pleistocene fan deposits sourced from the catchments as they drained into the old Fucino lake (Fig. 1c; *Accordi et al., 1986; Cavinato, 1993; Cavinato et al., 2002*). Because the indurated nature of these deposits precluded in-situ grain-size evaluation by sieving or in-situ Wolman point counts, we have estimated the coarse fraction sediment calibre in these cases using scaled grain-size photographs of the exposures perpendicular to bedding. A graticule was imposed onto the image in *Adobe Photoshop*© and the largest visible diameter of clasts lying on each of 100 grid intersection points was measured (c.f. *Cowie et al., 2008*). Empirically, the smallest clasts that could be accurately measured from such photographs were ~3 mm in diameter. This methodology approximately replicates the Wolman approach, and comparisons between such measurements and image-derived estimates of median grain-size on modern gravel bars are typically good (e.g. *Attal & Lavé, 2006*). Nevertheless, there is inherently some under-estimation of grain-size in this type of analysis because the measured diameter depends on the orientation of the clasts relative to the exposure plane. In the scenario where every pebble long-axis is oriented out of the plane of the photograph, the visible clast diameter will be the intermediate axis, which we determined to be ~30% smaller, on average, for carbonate clasts in this study area. This gives an upper bound to the errors associated with the approach, although we stress that we tried to avoid exposures that were oriented such that this was a significant problem.

4. Results

4.1 Morphology, locus and volume of sediment exported from transient catchments

Fig. 3 shows both hill-shaded images and catchment boundaries, derived from a 20m resolution DEM of the Central Apennines, for the rivers whose convex long profiles are shown in Fig. 2a. These channels all cross faults that have increased their uplift rate at 0.8 Ma, and in each of these cases the convex, high gradient reach in the river long profile above the active fault is associated with a prominent incised zone in the topography, with steep, rejuvenated hillslopes directly coupled to the channel. We have mapped a number of large landslides (green dots, Fig. 3) directly feeding into the channels within these reaches. The top of this incised zone (hill-shade image - thick white dashes) is separated from the upper part of the catchment by a pronounced break in slope. In contrast, the headwaters of these catchments are generally of low gradient, with wide valleys and gently dipping hill-slopes that are not affected by landsliding and are not deeply incised (see also *Whittaker et al., 2007b*). This is particularly clear in the catchments in the footwall of the Fucino fault (Fig. 3c, d) which has had the greatest tectonic perturbation (it is important to stress that the flat area at the top of Gole di Celano (Fig. 3c) is not an artefact of filling the DEM).

The fact that much of the incision within these catchments is taking place in a narrow zone upstream of the fault immediately challenges the idea that sediment supplied to hanging-wall basins downstream of active faults is sourced uniformly from hinterland catchments. Instead, the locus of sediment production is in the incised transient reach, which represents 5 to 40% of the total catchment drainage area (Table 1). Consequently the rate of sediment generation is unrelated to drainage area. Assuming the catchments were in topographic steady-state prior to the increase in uplift rate at 0.8 Ma, we can estimate, to first order, the total additional amount of sediment that has been removed from the catchment by simply projecting the concave part of the long profile upstream of the slope break downstream to the fault, and calculating the volume of space beneath this surface elevation in ArcGIS (Table 1). Panels on the right in Fig. 3 show contours of apparent incision below the break in slope calculated as a result of this estimation. These contours emphasize that the modern day catchments have been incised by several hundred metres since the uplift rate on the faults increased, and graphically demonstrate how continued fluvial erosion has rejuvenated hill-slopes to angles ≥ 35 degrees within the transient reach. Estimates of additional sediment volume produced from this incised zone, due to the transient response to slip rate increase on the faults range from 0.05 to 2.5 km^3 (Table 1). Moreover, values produced by the simple method above are probably under-estimates because the total volume will be substantially reduced by any sediment accumulation in the hanging-wall of the fault, and will also depend on the exact spatial distribution of uplift in the normal fault block. These factors can be geometrically corrected if we multiply the increase in slip-rate by the time since fault acceleration, to estimate the additional total throw on the fault produced in the transient phase. If this height is linearly projected to the elevation of the slope break in the catchment, then the volume of space within the catchment boundary below this surface gives a an upper estimate to the total incised volume. This correction makes little difference for the Torrente L'Apa and La Canala, but allows us to put maximum bounds on the additional volume of sediment produced in the transient phase for the Rio Torto (1.6 km^3), Gole di Celano (2.5 km^3) and Rio di Aielli (3.5 km^3). These values suggest that a substantial increase in sediment output from catchments to hanging-wall basins, derived from a limited source area, is to be expected as bedrock rivers in upland areas adjust to changes in their tectonic boundary conditions (see section 5.1 for further discussion).

4.2 Downstream changes in sediment calibre.

The transient response to fault uplift is clearly associated with additional production and export of sediment from discrete sources over time. However, is this simply a volume signal, or does the additional sediment also have different grain-size characteristics? Figure 4 shows gravel-bar grain-size derived from Wolman point counts along the main stem of the five catchments shown in Fig. 3. The grey box in each diagram corresponds to the incised zone upstream of the fault and downstream of the break in slope in the long-profile, where the channel is responding to the change in fault uplift rate. For all five catchments, there is little trend in median grain-size (D_{50}), with D_{50} almost always < 5 cm. However, for all of the catchments except La Canala (Pescasseroli fault), the incised zone with high channel gradients is characterised by elevated coarse fraction D_{84} grain-sizes that peak at or near the active fault. This zone of elevated D_{84} corresponds to the zone where we have mapped numerous large landslides (Fig. 3). This signal is even more pronounced when we calculate D_{50} and D_{84} using the more robust, but time consuming, weighted grain-size analysis. For the Celano and Rio Torto catchments (Fig. 5) we see D_{84} values which peak at > 20 cm. Maximum values are therefore an order of magnitude larger than those documented upstream of convex reach, i.e. in the area which has not yet responded to the increase in fault uplift rate. Weighted D_{50} values show a more muted response, with typical grain-sizes within the transient reach of ~5 cm in both cases, but lower in the upstream headwaters by a factor of > 2. We note that while there is reasonable correspondence between Wolman and weighted grain-size methods in the Celano catchment, for the Rio Torto, which crosses the Fiamignano fault, D_{84} appears to differ by a factor of 2. This problem affects D_{50} also, but to a much lesser extent. The discrepancy is most easily explained if the surface layer in the Rio Torto, when it was measured during the summer, was finer than the sub-surface that is accessed for weighted grain-size measurements, because recent low flow had deposited a veneer of finer gravel onto coarser gravel bars.

A key question is how the magnitude of the documented grain-size response compares (i) between channels with different degrees of tectonic perturbation, and (ii) with respect to rivers crossing faults, but which have reached topographic steady state? Fig. 6 shows both median and coarse fraction grain-size derived from Wolman point counts, normalised for distance to the fault, for two channels crossing faults which have moved at a constant slip rate for at least 3 My (Fig. 1; *Whittaker et al.*, 2007b). These channels erode identical lithology, but do not have convex reaches in the long profile and do not form gorges upstream of the fault (Fig. 3). Here D_{50} and D_{84} is approximately constant downstream, with no peak in coarse fraction grain-size near the fault. The differing grain-size signals between the channels are not a result of differing catchment size or tributary inputs: the Valleluce river (circles, Fig. 6) has $A = 20$ km^2, similar to La Canala (Fig. 4a) while the Fosso Tascino (triangles, Fig. 6) has $A = 42$ km^2, similar to the Gole di Celano (Fig. 4e) which has a significant long profile convexity (Fig. 3a) and a peak in D_{84} upstream of the fault. Moreover, in each of the transient cases, the intial increase in coarse fraction grain-size coincides with the top of the convex reach in the long profile, and not with any tributary (indeed, for the Gole di Celano, there are no tributaries within the incised reach).

However, the sediment calibre exported from the channel is related to the degree to which the catchment is perturbed from tectonic steady-state. La Canala (Fig. 4a), which crosses the Pescasseroli fault, has undergone the smallest relative tectonic perturbation since 0.8 My, an uplift rate increase of ~ 0.15 mm/yr (i.e. a 1.5 fold increase in slip rate on the fault). This has resulted in the development of a small steepened reach and incised zone (Fig. 3e) that does not have a significantly elevated grain-size compared to the upstream section of the catchment. In contrast the Gole di Celano, which has seen a five fold increase in uplift rate (present day rate = 1.5 mm/yr), has a very significant grain-size spike in the gorge upstream of the fault, particularly with respect to the coarse fraction. Fig. 7 shows both maximum D_{84} and average D_{84} in the 2 km upstream of the fault as a function of the slip-rate perturbation. For these seven catchments crossing uniform limestone lithology and with $18 < A < 62$ km^2, the size of the coarse-fraction grain-size peak upstream of the fault is positively correlated with the amplitude tectonic perturbation - an increase of 3-6 times in D_{84} over the range of slip-rates considered here. In contrast, the signal for median grain-size is much less clear, and several catchments (e.g. Rio Torto, Rio di Aielli and Celano) display significant increases in D_{84} while D_{50} does not vary greatly. The disparity between average and coarse fraction grain-size therefore increases within the transient, incised reaches upstream of the fault. While the constant slip rate Fosso Tascino and the Valleluce catchments maintain a constant D_{84}-to-D_{50} ratio of ~2, (a ratio which is typically replicated both downstream of the active fault and upstream of the gorges for the transient examples as well), D_{84} can be as much as 3-4 times larger than the median grain-size for catchments which have undergone a significant tectonic perturbation.

The origin of the grain-size signal can be seen in the cumulative frequency graphs (Fig. 8) of the weighted sediment grain-size measurements for these two catchments, from which D_{50} and D_{84} presented in Fig. 5 are derived. Results are presented in terms of downstream distance, L, relative to the position of the fault, L_f, and sediment exported from the upper part of the catchments (i.e. $L/L_f < 0.45$; black dashes) are generally gravels characterized by a unimodal grain-size distribution. However, as the steep, incised zone upstream of the fault is reached in both cases ($0.45 < L/L_f < 0.7$; black dots), the upper tail of the cumulative frequency curves spreads towards coarser grain-sizes. This allows for substantial increases in D_{84} without very large changes in the median calibre of the sediment in transport. Near the fault, ($0.7 < L/L_f < 1$; black lines), the sediment distribution is often bi-modal, with a second peak in the cobble grain-size class. These cobbles are progressively lost from the system beyond the faults ($L_f > 1$; grey dashes/lines) as the gradient of the channel bed abruptly falls (Fig. 2), re-establishing a unimodal grain-size distribution with $D_{84}/ D_{50} \sim 2$.

Our data also allow us to evaluate the distance over which the coarse fraction grain-size propagates downstream beyond the fault. For the Rio di Aielli and Celano catchments entering the internally drained Fucino basin, D_{84} decays rapidly in the hanging-wall of the fault, with the coarse fraction grain-size signal attenuated in less than 2 km (Fig. 4d, e, Fig. 5a) and the gravel front (*sensu* Sambrook Smith & Ferguson, 1995) lying less than 3 km beyond the fault. This is mirrored for the Rio Torto, where coarse fraction grain-size decays rapidly (e.g. by a factor of 4 within ~3 km) for both Wolman or weighted sediment methodologies. By the time the channel enters the main axial river at 15.8 km downstream, sediment exported from the modern day channel has returned to a unimodal grain-size distribution, with D_{84} being approximately twice the size of D_{50}, although here we do not lose the gravel from the system entirely. Only in the case of the Torrente L'Apa, where the axial river lies close to the fault, do coarse sediments enter a large river system that transport them over longer distances.

5. Discussion.

5.1 Sediment release from transient catchments

The data presented above show that for channels eroding limestones in the Central Apennines of Italy, the transient response to an increase in fault uplift rate is associated with:

(i) an increase in the total volume of sediment supplied to neighbouring basins as the catchments adjust to the new slip rate on the fault. For catchments with drainage areas of ~40 km^2 which have increased their slip rate by ~1.5 mm/y at 0.8 Ma, the additional material removed from each catchment is of the order of 3 km^3.

(ii) the development of a discrete locus of incision upstream of the fault resulting in a strongly non-uniform distribution of sediment production within the catchment.

(iii) the transport of sediment within the incised, transient reach of the catchments that has a significant peak in coarse fraction D_{84} grain-size. This is relative both to the sediment supplied from the upstream headwaters of the catchments that have not yet detected the change in fault uplift rate, and the sediment transported through similar catchments that have reached topographic steady-state. The magnitude of this signal is correlated to the degree of tectonic perturbation.

These results are important because they demonstrate that the sediment released from catchments undergoing a transient response to tectonics is sourced from discrete areas, with discrete characteristics over a discrete period of time. Our findings therefore provide direct field confirmation of recent numerical modelling studies (*Hardy & Gawthorpe,* 2002; *Cowie et al.,* 2006), whose outputs suggest that transient responses should be associated with significant export of sediment from localised areas, although their models contains no information about the characteristics of the sediment yielded. How significant is this extra supply of sediment in absolute volume terms? A 40 km^2 catchment that had reached topographic steady-state with respect to an uplift rate of 0.3 mm/yr would require the erosional removal of ~9.6 km^3 of material across the landscape over a period of 0.8 My, assuming a uniform rate of erosion across the catchment area. For the more realistic case of a back-tilted normal fault block, where the uplift rate falls to zero at a fulcrum situated in the headwaters of the catchment, we would need to erode ~4.8 km^3 of rock over the same time period, assuming drainage area is evenly distributed within the footwall. However, for all our catchments, a disproportionate area is located in the distal footwall (60-70%), with little drainage area near the fault. This reduces the volume to be eroded to < 3 km^2 over a 0.8 My time period for an uplift rate of 0.3 mm/yr. In comparison, our estimates of the *additional* volume removed from catchments of this size crossing the Fucino fault, which have been perturbed by a significant increase in uplift rate, suggest that an additional 3 km^3 have been exported, i.e. 100% of the above totals; these figures will increase as the transient wave of incision continues to propagate through the catchment. These figures show that not only is there a significant pulse in the total volume of sediment exported to neighbouring depositional basins during the transient phase, but also that much of it is sourced from near the fault. Moreover, the fact that sediment is not derived uniformly across the catchment as a function of drainage area underlines the inherent dangers for any studies attempting to derive catchment wide erosion rates from sediment samples using cosmogenic nucleides (c.f. Gayer et al., 2008) in tectonically active areas.

Finally, the response is likely associated with a change in the shape of the probability distribution of sediment volume released from the catchment over a selected time frame (e.g. per event, per year, etc) as averaged over any arbitrary longer period. This is because transient channels crossing faults are significantly steeper upstream of the fault (by a factor > 5 in some cases) compared to those that have reached topographic steady-state and have concave long profiles (see long profiles, Fig. 2; *Whittaker et al.*, 2007b). Consequently their absolute capacity to transport sediment, Q_t, is substantially increased: e.g. the simple Meyer-Peter Muller (1948) long term transport capacity estimation, $Q_t \sim S^{1.5}$, implies that a slope increase by a factor of 5 increases Q_t by a factor > 10. The implication of this is that the spread in the *pdf* of sediment volume exported within any given time period must also increase, because the ability of the river system to move material is actually much larger than the additional volume of sediment eroded as the river adjusts to the new uplift rate on the fault i.e. the system becomes highly undersupplied with respect to sediment input (c.f. *Gasparini et al.*, 2007).

5.2 What process best explains the elevated grain-size signal?

Our results show that sediment export from catchments undergoing a transient response to tectonics is associated with a significant peak in the coarse fraction grain-size of material in transit upstream of the fault. The magnitude of this coarse fraction peak grows with increasing degree of tectonic perturbation (Fig. 7) and is associated with significant disparity in the D_{84}-to-D_{50} ratio which is apparently related to the development of bi-modal grain-size distribution within the channel (Fig. 8). Bi-modal grain-size distributions in upland mountain catchments are typically related to the existence of sources providing sediment of markedly different calibre to the channel (e.g. *Radoane et al.*, 2007). The grain-size trend is not related to changing bedrock type or tributary inputs, but instead is directly correlated with the wave of incisional rejuvenation that is propagating up the catchment in response to the increase in fault uplift rate. The propagation of this signal has resulted in the formation of significant gorges upstream of the active faults, and is clearly associated with the input of many large landslides directly into the channel (Fig. 3). We therefore hypothesise that the grain-size signal is a direct product of the close coupling between hill-slope processes and channel incision that has developed in the incised reach as a result of the increase in fault uplift rate.

To test this hypothesis, we investigated the extent to which the grain-size distribution of sediment supplied to the channel could account for the signal seen. We therefore analysed the calibre of sediment from five landslides and scree cones that feed directly into the Rio Torto (Fig. 9a), the best characterised of the channels undergoing a transient response to tectonics (*Whittaker et al.*, 2007a). The two landslides sampled appear to have similar grain-size distribution than the sediment in the channel at the finer end of the spectrum (cumulative frequency < 0.5) but have coarser grain-size tails. Scree cones are much more variable, but are a significant source of coarse fraction debris (e.g. cone 5). We note that much of the river upstream of the fault, but downstream of the break in slope in the long profile is fed by these cones (Fig. 9b). The landslide distributions are finer than those measured by Casagli *et al.* (2003) for deposits in the Northern Apennines sourced from a similar lithology, but we note that they contain boulders within their sediment calibre analysis which, although abundant in our case also, are impossible to include without requiring several tonnes of sediment to be sieved and weighed at each locality. Even withstanding this, it is clear that sediment that is supplied from hill-slope processes is substantially coarser than that which is supplied from upstream in the channel (grey dashes; Fig. 9a), particularly with respect to the coarse fraction. Given that these landslides and scree cones are typical source of sediment from hill-slopes throughout this part of Italy, we therefore interpret the grain-size signal we have documented to be the result of a strong coupling between tectonically driven river incision, and the hill-slope response to this (c.f. *Densmore et al.,* 1998; *Schuerch et al.,* 2006). This is in contrast to channels which have already reached topographic steady-state with respect to on-going fault uplift, which have concave up long profiles, do not display rejuvenated, steepened hill-slopes bounding the channel near the fault, and hence do not have significant landslide input directly to the axial channel (which is required to boost coarse fraction grain-size in the channel).

However, we have also shown (Fig. 7) that there is a correlation between the degree of tectonic perturbation and the magnitude of the D_{84} signal. While it is true that the maximum channel gradients upstream of the active faults do increase to some extent with the fault slip rate (Fig. 2), there is no direct relationship between grain-size in the channel and long profile slope. Moreover, these channels are significantly under-supplied with sediment with respect to their transport capacity, with Shield stresses more than an order of magnitude larger than one would expect for a transport-limited gravel bed river (see *Whittaker et al.,* 2007b*; c.f. Mueller & Pitlick,* 2005), implying that much of the sediment in the channel, regardless of size, must be mobilised at high flow. This means the increase in grain-size found in the channel with fault uplift rate cannot be simply explained by a call to stream-wise river gradient (c.f. *Wohl*, 2004; *Whittaker et al.*, 2007a). Significantly, we also note that La Canala, crossing the Pescasseroli fault, which has undergone the smallest degree of tectonic perturbation, and has the most limited incised zone, with few landslides, does not display any elevated grain-size signal within the transient reach. We therefore contend that the grain-size signal only starts to develop once the threshold for landsliding, particularly bedrock landsliding, is exceeded (*Densmore et al.*, 1998; *Lavé & Burbank*, 2004; *Korup & Schlunegger*, 2007; *Ouimet et al.*, 2007). Hillslopes in the Pescasseroli case are typically less than 20 degrees, whilst in the Torrente L'Apa, which has undergone a marginally larger degree of slip rate increase and does have a number of large landslides feeding the channel, there is a 1 km zone upstream of the fault where the channel is incised vertically by approximately 200 m over ~300-400 m of plan-view distance, as measured from the break in slope in the hillside (Fig. 3b), giving hill-slope angles of ~28-38 degrees. The exact threshold angle needed to initiate landsliding will depend on the precise lithological strength and the degree of rock fracturing in each case, but it seems for the fractured carbonates in this area, hillslope gradients of ~30 degrees are sufficient to initiate landsliding, which is similar to values obtained for experimental work with granular media (*Roering et al.*, 2001). The increase in coarse fraction grain-size beyond this point with increasing degree of slip rate perturbation on the fault (Fig. 7) is then best explained by either:

(i) larger landslides, which also happen to contain larger clasts, enter channels crossing faults which have higher slip-rates and are down-cutting more rapidly;

(ii) more frequent landslides occur within the transient incised zone for channels crossing higher slip-rate faults. In this case, as all channels are strongly under-supplied in the headwaters, the proportion of relatively coarse sediment derived from landsliding near the fault becomes greater with respect to sediment fluxed from above the transient incised zone as the slip rate increases. This effect will occur both because more landslides are required per unit time to keep pace with greater rates of fault uplift and hence river incision, and because the extent of the incised zone is larger within catchments experiencing higher uplift rates (Fig. 3) and hence will garner more hill-slope derived sediment. Both (i) and (ii) are not mutually exclusive, although we do not have the data for this area of Italy to show that landslides of larger volume demonstrably supply larger clasts to the river system.

5.3 What effect does transient response have on depositional stratigraphy?

The data presented above demonstrate that a transient response to tectonics has a significant impact on the *pdf* of sediment grain-size exported from upland catchments, particularly with respect to the coarse fraction. This should have a substantial impact on depositional stratigraphy, as the calibre and quantity of sediment exported from catchments helps determine the characteristics and locus of sedimentary deposits preserved within neigbouring basins. However, the length-scale over which the coarse fraction grain-size signal remains detectable in the modern Italian river sediments studied here is only 2-3 km downstream of the active faults. Moreover, for the Celano and Aielli catchments, which have the greatest uplift rates, but concomitantly the most rapid generation of accommodation space in the hanging-wall, no gravel is transported more than ~ 4 km downstream of the active fault. Only in the case of the Torrente L'Apa does a river sourced from a catchment responding transiently to tectonics actually supply coarse material to a large axial channel (in this case with a drainage area > 100 km^2) which is capable of exporting this material over long distances. The above observations suggest that (i) the grain-size signal produced by a transient response to tectonics is only likely to be exported over a long wavelength if catchments undergoing such a perturbation drain into a large axial river (i.e. with significant transport capacity) that lies close to the fault bounded mountain front, and hence (ii) that transient responses to tectonics are much more likely to be recorded in the proximal stratigraphy of hanging-wall basins. This signal should be magnified for catchment-basin systems that have undergone a larger degree of tectonic perturbation, because the grain-sizes produced within the transient reach are likely to be coarse, while the high rate of tectonic subsidence downstream of the fault promotes rapid sediment deposition.

We evaluate these effects by considering the stratigraphy of the Fucino basin, which forms the hanging wall to the Fucino fault (Fig. 1; Fig. 10a) and is sourced at its north-eastern margin by the Gole di Celano and the Rio di Aielli, as well as a number of other rivers. This internally-drained basin was a lake until its draining in the late 19th century, and these two rivers have built out substantial Pleistocene-to-Recent low-gradient fans into the basin, some of which are now exposed between the Northern active fault strand and the old lake margin (circles in Fig. 10a., see also *Cavinato et al.*, 2002*; Roberts & Michetti*, 2004). Additionally, seismic lines and boreholes presented by Cavinato *et al.* (2002) give excellent constraints on the basin stratigraphy and timing of sediment deposition (Fig. 10b). Significantly, sequence 3, of upper Pliocene-lower Pleistocene age, deposited before the bounding Fucino fault linked and hence increased its slip rate, is dominated by moderate grain-size alluvial fan, lake delta and some shallow lake deposits. Moreover, the thickness is only 250 m, while the time taken for deposition is > 1 My. Conversely, deposits of upper Pleistocene age (sequence 4b) form fine, uniform alternations of siltstone and mudstone layers extending across the basin, with a documented 0.5 Ma tephra layer at only 100 m depth implying significant empty accommodation space given that modern-day throw rate estimates are up to 1.5mm/yr for this locality (*Cavinato et al.*, 2002; *Roberts & Michetti*, 2004; *Whittaker et al.*, 2008). The basin has therefore transitioned from approximately filled during the early Pleistocene to under-filled by the upper Pleistocene. On first sight, these findings present a potential paradox, because fault acceleration is associated both with an increase in the volume of sediment being exported from the catchments bounding the basin, and also a significant increase in the calibre of material being exported. This apparent paradox is resolved by considering the timing and locus of the erosional response to tectonic forcing. Firstly, the response to the uplift rate increase propagates relatively slowly upstream of the fault (8-10 mm/yr: *Whittaker et al., 2008*), meaning that while part of the catchments has adjusted to the increase in fault uplift rate, the headwaters are yet to "detect" the change in relative base level. Consequently it takes time for the volume of sediment output to increase; in contrast the increase in hanging-wall subsidence rate is felt immediately across the whole basin (*Hardy & Gawthorpe,* 2002*; Cowie et al.,* 2006). These observations require that much of the coarse fraction sediment derived from erosion since the fault acceleration must be stored in fans just downstream of the Fucino fault, as the basin is internally drained and the sediment has to be deposited somewhere. This is exactly what we see for mapped upper Pleistocene proximal fan deposits exposed near the Rio di Aielli and Gole di Celano, (Fig. 10a, c; *Accordi et al.,* 1986). Although limited exposure and the presence of numerous small normal faults does not allow grain-size to be reconstructed for individual timelines downstream, the majority of these deposits are coarse with 5.5 cm < D_{84} < 12 cm for the Aielli fans, and 5 cm < D_{84} < 18 cm for the Celano example (Fig. 10c). Additionally, we also documented examples in the same area of thin gravels (grey dashed lines in Fig. 10c) which are interbedded with lacustrine units in the vicinity of Aielli Stazione and Cerchio (Fig. 9; see also *Cavinato et al.*, 2002) showing these fans fed directly into the nearby lake. Given the rapid grain size fining that is documented for the modern systems downstream of the fault (e.g. Fig. 4d, e), it is clear that deposition, and hence removal from the fluvial sediment load, of sediments with grain-size distributions similar to those in Fig. 10c, will produce the rapid modern fining downstream, which would be impossible to achieve by other processes such as abrasion, over such short length scales (*Attal & Lavé, 2006*).

5.4 Wider implications and research needs

These results have a wide significance for both geomorphologists seeking to understand the coupling between uplift, river incision and hill-slope responses, and for sedimentologists looking to understand the impact of sediment production and export on depositional stratigraphy. Our results show that transient landscape response to tectonics controls the locus, magnitude and characteristics of sediment export from upland catchments, while the interplay between the generation of uplift and accommodation space, relative to the erosional response timescale determines the relative position and distribution of grain-sizes preserved in the hanging-wall basins. Such insights help to explain why, for internally drained basins, the timing of fault interaction may be marked by a transition to fine grained, even lacustrine sediments, as erosional response lags behind accommodation generation. In a similar way, our results highlight the danger of interpreting an influx of gravels or pebbles into a basin as simply a switch to "higher energy environments" or as proof of landscape response to climatic changes (c.f. *Heller and Paola, 1992*). In Fig. 11 we show a synthesis of the coupled response of tectonics, erosion and sedimentation as evidenced in the Central Apennines.

How widely applicable are these findings? Strictly our results concern terrestrial catchments draining relatively hard bedrock footwalls whose erosional behaviour lies towards the detachment-limited end member (*Whittaker et al.,* 2007b, *Cowie et al.,* 2008). Softer footwall lithologies such as poorly consolidated sandstone or schist are likely to produce rather different responses for two reasons. Firstly, even if the catchment did respond in a "detachment-limited" way, the response time of the poorly resistant bedrock would be shorter, so the increase in sediment flux per unit time would be greater, while the distribution of grain-sizes exported during the transient phase would also be finer, since the clasts supplied by hill-slopes would be quickly reduced in size by abrasion (*Attal & Lavé*, 2006). Secondly, it is likely that the erosional process would differ too. Examples of channels crossing faults in Greece, presented in Cowie et *al.*, (*2008*), demonstrate that the presence of lacustrine and gravel beds in the footwall stratigraphy promotes a more diffusive landscape response (i.e. sediment-flux mediated *sensu Sklar & Dietrich,* 2004) without the development of large long profile convexities. In this case, where the rivers are responding to a similar tectonic perturbation in both space and time to the Italian examples presented here, incision has also propagated to the top of the catchment, arguing for shorter landscape response times and hence a larger quantity of sediment flux per unit time. A key research need is therefore for studies which calibrate transient channel response times and grain-size export for differing lithologies and erosional process. Indeed, these results already suggest that the coupling between uplift and erosion in upland catchments is likely to dynamically affect the rate and style of fluvial erosion, as the onset of landsliding in the transient part of steep footwall catchments provides a significant source of sediment in addition to the material being supplied from upstream. The input rate and magnitude of this "new" source relative to the long term transport capacity of the system will determine the dominant fluvial erosion process and could either enhance or reduce incision rates accordingly (*Sklar & Dietrich*, 2004*; Gasparini et al.,* 2006*; Cowie et al.,* 2008).

The variability in the quantity and volume of sediment being sourced from these catchments will also affect the sediment deposited in neighbouring hanging-wall basins. However, we believe that many of our generic conclusions relating to basin sedimentation hold. Firstly, any coarse sediment is likely to end up in the proximal hanging-wall unless there is significant axial transport, and secondly that in terrestrial rift settings there is likely to be a time-lag between the generation of accommodation space due to an increase in fault uplift rate and the erosional response which should be detectable in the hanging-wall basin stratigraphy. However, for softer lithologies with a shorter erosional response timescale, this signal will be more muted and may not be accompanied by the progradation of relatively coarse grain-size fans in the proximal part of the basin. The recognition of 'transient stratigraphy' in normal fault bounded basins with varying lithologies and temporal history of slip remains a significant challenge for the future.

6. Conclusions.

In this paper, we address the important question of where, how and with what characteristics sediment is released from catchments in response to tectonic perturbation, using case studies of rivers crossing active normal faults in the Central Apennines of Italy. We show that for under-supplied bedrock rivers (i.e. those close to the detachment limited end-member) responding to an increase in fault uplift rate at 0.8 Ma, erosion is mostly localised in an actively incising zone upstream of the fault. Sediment export from these catchments, which incise hard carbonate bedrock, is characterised by the presence of significant coarse fraction grain-sizes (typical D_{84} ~10 cm) that are substantially derived from coupled hill-slopes sediment supply; our field observations also show that the amplitude of this response is modulated by the degree of tectonic perturbation. In contrast, catchments crossing faults which have not changed their slip rate over time and have reached topographic steady-state (*Whittaker et al.*, 2007b) do not display this grainsize signal. Sediment volumes exported from the incised transient reaches vary in a non-linear way with fault slip rate, but are documented to be > 3 km^3 for catchments of 30-40 km^2 areal extent, and crossing faults which have undergone a five-fold slip rate increase to ~1.5 mm/yr.

In the neighbouring hanging-wall basins, the grain-size in the modern day channels decreases rapidly downstream, with a loss of almost all coarse sediment > 4 cm within 3-6 km beyond the active fault. These results show that coarse fraction grain-sizes are likely to be locked up preferentially in proximal hanging-wall stratigraphy, except if a large axial river drains close to the footwall and can thus potentially export the coarse material further down the fluvial network. Our conclusions are supported by seismic data and analysis of upper Pleistocene fans in the Fucino Basin and show that 'transient' hanging-wall stratigraphy is explicitly controlled by the balance between uplift, accommodation generation, and the length and timescale of the erosional response. More widely, our results challenge the view the sediment is sourced uniformly from tectonically active catchments and demonstrate that a detailed understanding of transient landscape responses to tectonic perturbation is required to understand both the locus, magnitude and calibre of sediment export from catchments, and also the distribution and characteristics of basin stratigraphy.

7. Acknowledgements

This work was supported by StatoilHydro (Whittaker, Allen) and NERC Research Grants NER/S/A/2002/10359 (Whittaker) and NE/B504165/1 (Attal). The authors are particularly grateful to Patience Cowie, Greg Tucker and Gerald Roberts, whose considerable contribution to recent work on the geomorphology of the Central Apennines provided the starting point for this study. We thank Zana Conway for her help in collecting field data and Eutizio Vittori for supplying the DEM.

8. References:

Accordi, G., Carbone, F., Civitelli, G., Corda, L., De Rita, D., Esu, D., Funicello, R., Kotsakis, T., Mariotti, G. & Sposato, A. (1986). Lithofacies map of Latium-Abruzzo and neighbouring areas, Consiglio Nazionale delle Ricerche, Italy.

Allen, P. A. (2008) From landscapes into geological history, *Nature*, **451**, 274 – 276.

Allen, P. A. (2007) Earth science - Sediment en route to oblivion, *Nature*, **450**, 490 – 491.

Allen, P. A. & Allen, J. R. (2005) Basin analysis: principles and applications, Oxford Blackwell Publishing, ISBN: 0-6320-5207-4.

Allen, P. A., & Densmore, A. L. (2000) Sediment flux from an uplifting fault block, *Basin Research*, **12**, 367-380.

Attal, M. & Lavé, J. (2006) Changes of bedload characteristics along the Marsyandi River (central Nepal): Implications for understanding hillslope sediment supply, sediment load evolution along fluvial networks, and denudation in active orogenic belts, *in* Willett, S.D., Hovius, N., Brandon, M.T., and Fisher, D., eds., Tectonics, Climate, and Landscape Evolution: *Geological Society of America Special Paper*, **398**, p. 143–171, doi: 10.1130/2006.2398(09).

Attal, M., Tucker, G.E., Whittaker, A.C., Cowie, P.A. & Roberts, G.P. (2008) Modelling fluvial incision and transient landscape evolution: influence of dynamic channel adjustment, *Journal of Geophysical Research*, **113**, F03013, doi:10.1029/2007JF000893.

Burbank, D. W. & Pinter, N. (1999) Landscape evolution: the interactions of tectonics and surface processes, *Basin Research*, **11**, 1-6.

Casagli, N., Ermini, L. & Rosati, G. (2003) Determining grain size distribution of the material composing landslide dams in the Northern Apennines: sampling and processing methods, *Engineering Geology*, **69**, 83-97.

Castelltort, S. & Van den Driessche, J. (2003) How plausible are high-frequency sediment supply-driven cycles in the stratigraphic record? *Sedimentary Geology*, **157**, 3-13.

Cavinato, G. P. (1993) Recent tectonic evolution of the quaternary deposits of the Rieti Basin (Central Apennines, Italy): Southern part, *Geologica Romana*, **29**, 411-434.

Cavinato, G. P. & DeCelles, P. G. (1999) Extensional basins in tectonically bi-modal central Apennines fold-thrust belt, Italy: Response to corner flow above a subducting slab in retrograde motion, *Geology*, **27**, 955-958.

Cavinato, G. P., Carusi, C., Dall'Asta, M., Miccadei, E. & Piacentini, T. (2002) Sedimentary and tectonic evolution of Plio–Pleistocene alluvial and lacustrine deposits of Fucino Basin (central Italy), *Sedimentary Geology*, **148**, 29–59.

Centamore, E. & Nisio, S. (2003) Effects of uplift and tilting in the Central-Northern Apennines, Italy, *Quaternary International*, **101-102**, 93-101.

Cowie, P. A., Whittaker A. C**.,** Attal, M., Tucker G. E., Roberts G. P. & Ganas, A. (2008) New constraints on sediment-flux dependent river incision: Implications for extracting tectonic signals from river profiles, *Geology*, **36**, 535–538; doi: 10.1130/G24681A.1.

Cowie, P. A., Attal, M., Tucker, G. E., Whittaker, A. C., Naylor, M., Ganas, A. & Roberts G. P. (2006) Investigating the Surface Process Response to Fault Interaction and Linkage Using a Numerical Modeling Approach, *Basin Research*, **18**, 231-266.

Cowie P. A. & Roberts, G. P. (2001) Constraining slip rates and spacings for active normal faults, *Journal of Structural Geology*, **23**, 1901-1915.

Dadson, S. J., Hovius, N., Chen, H., Dade, W. B., Hsieh, M., Willett, S. D, Hu, J, Horng, J., Chen, M., Stark, C. P., Lague, D. & Lin, J. (2003) Links between erosion, runoff variability and seismicity in the Taiwan orogen, *Nature*, **426**, 648-651.

D'Agostino, N., Jackson, J. A., Dramis F. & Funiciello, R. (2001) Interactions between mantle upwelling, drainage evolution and active normal faulting: an example from the central Apennines (Italy), *Geophysical Journal International*, **147**, 475-497.

D'Agostino, N. & Jackson, J. A. (1999) Convective support of long-wavelength topography in the Apennines (Italy), *Terra Nova*, **11**, 234-238.

Densmore, A. L., Allen, P. A. & Simpson, G., (2007). Development and response of a coupled catchment fan system under changing tectonic and climatic forcing, *Journal of Geophysical Research*, **112**, F01002, doi: 10.1029/2006JF000474.

Densmore, A. L., Ellis, M. A. & Anderson, R. S. (1998) Landsliding and the evolution of normal fault bounded mountains, *Journal of Geophysical Research*, **103**, B7, 15203-1521.

Elliot, P. P. & Gawthorpe, R. L. (1995) Drainage development and sediment supply within rifts, examples from the Sperchios basin, Central Greece. *Journal of Geological Society, London*, **152**, 883-893.

Gawthorpe, R. L. & Leeder, M. R. (2000) Tectono-sedimentary evolution of active extensional basins, *Basin Research*, **12**, 195-218.

Gasparini, N. M., Bras, R. L. & Whipple, K. X. (2006) Numerical modelling of non-steady-state river profile evoluton using a sediment-flux-dependent incision model, in Tectonics, Climate and Landscape Evolution Eds. S. Willet, N. Hovius, M. Brandon & D Fisher, *Geological Society of America Special Paper*, **398**, 127-141.

Gayer, G., Mukhopadhyay S. & Meade, B. J. (2008) Spatial variability of erosion rates inferred from the frequency distribution of cosmogenic ^{3}He in olivines from Hawaiian river sediments, *Earth and Planetary Science Letters*, **266**, 303-315, doi:10.1016/j.epsl.2007.11.019.

Hardy, S. & Gawthorpe, R. (2002) Normal fault control on bedrock channel incision and sediment supply: insights from numerical modelling, *Journal of Geophysical Research*, **107**, B10, 2246, doi 10.1029/2001JB000166.

Heller, P. L. & Paola, C. (1992) The large scale dynamics of grain-size variation in alluvial basins, 2: Application to syntectonic conglomerate, *Basin Research*, **4**, 91-102.

Hovius, N. & Leeder, M. (1998) Clastic sediment supply to basins, *Basin Research*, **10**, 1-5.

Hovius, N., Stark, C. P., Hao-Tsu, C. & Jiun-Chuan, L. (2000) Supply and Removal of Sediment in a Landslide-Dominated Mountain Belt: Central Range, Taiwan, *Journal of Geology*, **108**, 73–89.

Horton, B. K., Constenius, K. N. & DeCelles, P. G. (2004) Tectonic control on coarse grained foreland-basin sequences: An example from the Cordilleran foreland basin, Utah, *Geology*, **32**, 637-640.

Kondolf, G.M. (1997) Application of the pebble count: notes on purpose, method, and variants, *Journal of the American Water Resources Association*, **33**, 79-87.

Korup, O. & Schlunegger, F. (2007) Bedrock landsliding, river incision, and transience of geomorphic hillslope-channel coupling: Evidence from inner gorges of the Swiss Alps. *Journal of Geophysical Research*, **112**, F03027, doi:10.1029/2006JF000710.

Lavé, J. & Burbank, D. (2004) Denudation processes and rates in the Transverse Ranges, southern California: Erosional response of a transitional landscape to external and anthropogenic forcing, *Journal of Geophysical Research*, **109**, F01006, doi:10.1029/2003JF000023.

Lavecchia, G., Brozzetti, F., Barchi, M., Menichetti, M. & Keller, J. V. A. (1994) Seismotectonic zoning in east-central Italy deduced from an analysis of the Neogene to present deformations and related stress fields: *Geological Society of America Bulletin*, **106**, 1107–1120.

Leeder, M. R., Harris, T. & Kirkby M. J. (1998) Sediment supply and climate change, implications for basin stratigraphy, *Basin Research*, **10**, 7-18.

Molnar, P. (2001) Climate change, flooding in arid environments and erosion rates, *Geology*, **29**, 1071-1074.

Montgomery, D. R. & Stolar, D. B. (2006) Reconsidering Himalayan Anticlines, *Geomorphology*, **86**, 4-15.

Morewood, N. C. & Roberts, G. P. (2002) Surface observations of active normal fault propagation: implications for growth, *Journal of the Geological Society, London*, **159**, 263–272.

Mudd, S. M. & Furbish, D. J. (2007) Responses of soil-mantled hillslopes to transient channel incision rates, *Journal of Geophysical Research*, **112**, F03S18, doi:10.1029, 2006JF000516.

Mueller, E. R. & Pitlick, J. (2005) Morphologically based model of bed load transport capacity in a headwater stream, *Journal of Geophysical Research*, **110**, F02016, doi:10.1029/2003JF000117.

Ouimet, W. B., Whipple, K. X., Royden, L. H., Sun, Z. & Chen, Z. (2007) The influence of large landslides on river incision in a transient landscape: Eastern margin of the Tibetan Plateau (Sichuan, China), *Geological Society of America Bulletin*, 119, 1462-1476, doi: 10.1130/B26136.1.

Palumbo, L., Benedetti, L., Bourles, D., Cinque, A. & Finkel, R. (2004) Slip history of the Magnola fault (Apennines, Central Italy) from Cl-36 surface exposure dating: evidence for strong earthquakes over the Holocene *Earth and Planetary Science Letters*, **225**, 163-176.

Paola C. & Swenson, J. B. (1998) Geometric constraints on composition of sediment derived from erosional landscapes, *Basin Research*, **10**, 37-47.

Patacca, E., Sartori, R. & Scandone, P. (1990) Tyrhhenian basin and Apenninic arcs: Kinematic relations since late Tortonian times, *Memorie della Societa Geological Italiana*, **45**, 425-451.

Pizzi, A., 2003. Plio-Quaternary uplift rates in the outer zone of the central Apennines fold and thrust belt, Italy. Quaternary International, 101-102, 229-237.

Radoane M., Radoane, R., Dumitriu, D. & Miclaus, C. (2007) Downstream variation in bed sediment size along the East Carpathian rivers: evidence of the role of sediment sources, *Earth Surface Processes and Landforms*, **33**, 674-694, doi:10.1002/esp.1568.

Roberts, G. P. & Michetti, A, M. (2004) Spatial and temporal variations in growth rates along active normal fault systems: an example from Lazio-Abruzzo, central Italy, *Journal of Structural Geology*, **26**, 339–376.

Robinson, R. A. J. & Slingerland, R. L. (1998) Grain-size trends, basin subsidence and sediment supply in the Campanian Castlegate Sandstone, and equivalent conglomerates of central Utah, *Basin Research*, **10**, 109-127.

Roering, J. J., Kirchner, J. W. & Dietrich W. E. (1999) Evidence for nonlinear, diffusive sediment transport on hillslopes and implications for landscape morphology, *Water Resources Research*, **35**, 853–870.

Roering, J. J., Kirchner, J. W., Sklar, L. S. & Dietrich, W, E. (2001) Hillslope evolution by nonlinear creep and landsliding: An experimental study, *Geology*, **29**, 143-146.

Sambrook Smith, G. H. & Ferguson, R. I. (1995) The gravel-sand transition along river channels, *Journal of Sedimentary Research*, **65**, 423-440.

Schlunegger, F. (2002) Impact of hill-slope derived sediment supply on drainage basin development in small watersheds at the northern border of the central Alps of Switzerland, *Geomorphology*, **46**, 285-305.

Schuerch, P., Densmore A. L., McArdell, B. W. & Molnar, P. (2006) The influence of landsliding on sediment supply in a steep mountain catchment, *Geomorphology*, **78**, 222-235.

Simpson, G. D. H. (2006) Modelling interactions between fold-thrust belt deformation, foreland flexure and surface mass transport, *Basin Research*, **18**, 125-143.

Sklar, L. & Dietrich, W. E. (2004) A mechanistic model for river incision into bedrock by saltating bed load, *Water Resources Research*, **40**, W06301, doi:10.1029/2003WR002496.

Stock, G. M., Ehlers, T. A. & Farley, K. A. (2006) Where does sediment come from? Quantifying catchment erosion with detrital apatite (U-Th)/He thermochronometry, *Geology*, **34**, 725-728.

Talling P. J. & Sowter, M. J. (1998) Erosion, deposition and basin-wide variations in stream power and bed shear stress, *Basin Research*, **10**, 87-108.

Tucker, G. E. & Slingerland, R. (1996) Predicting sediment flux from fold and thrust belts, *Basin Research*, **8**, 329-349.

Tucker, G. E., Bras, R. L. (1998) Hillslope processes, drainage density and landscape morphology, *Water Resources Research*, **34**, 2751-2764.

Tucker, G. E. & Whipple K. X. (2002) Topographic outcomes predicted by stream erosion models: Sensitivity analysis and inter-model comparison, *Journal of Geophysical Research*, **107**, 2179, DOI: 10.129/2001JB000162.

Weltje, G. J., Meijer, X. D. & De Boer, P. L. (1998) Stratigraphic inversion of siliciclastic basin fills : a note on the distinction between supply signals resulting from tectonic and climatic forcing, *Basin Research*, **10**, 129-153.

Whipple, K. X. (2004) Bedrock rivers and the geomorphology of active orogens, *Annual Review of Earth and Planetary Sciences*, **32**, 151-185.

Whipple, K.X. & Tucker, G.E. (2002) Implications of sediment-flux dependent river incision models for landscape evolution, *Journal of Geophysical Research*, **107(B2),** DOI: 10.1029/2000JB000044.

Whipple, K. X. & Tucker, G. E. (1999) Dynamics of the stream power incision model: Implications for the height limits of mountain ranges, landscape response timescales and research needs, *Journal of Geophysical Research*, **104**, 17,661-17674.

Whittaker, A. C., Attal, M., Cowie P. A., Tucker G.E. & Roberts, G. (2008) Decoding temporal and spatial patterns of fault uplift using transient river long-profiles, *Geomorphology*, **100**, 506–526, doi:10.1016/j.geomorph.2008.01.018.

Whittaker, A. C., Cowie, P. A., Attal, M., Tucker, G. E. & Roberts, G. (2007a) Bedrock channel adjustment to tectonic forcing: Implications for predicting river incision rates, *Geology*, **35**, 103-106.

Whittaker, A. C., Cowie, P. A., Attal, M., Tucker, G. E. & Roberts, G. (2007b) Characterizing the transient response of rivers crossing active normal faults: New field observations from Italy, *Basin Research*, **19**, 529-556, doi:10.1111/j.1365-2117.2007.00337.

Willett, S. D. & Brandon, M. T. (2002) On steady states in mountain belts, G*eology*, **30,** 175-178.

Figure Captions

Figure 1 (a) Inset map of Italy showing documented active normal faults. Grey box depicts study area shown in detail in Fig. 1b. **(b)** Geological and structural map of the Central Apennines, showing the location of thrusts and normal faults, and their relation to lithology. Active normal faults that increased their slip rate within the last 1 My are shown in red; other normal faults are shown in black. **(c)** DEM derived image of the Central Apennines (resolution 20 m), showing the rivers (blue) and the associated active normal fault systems referred to in this study. Increased slip-rate faults are shown in red; faults which have had a constant slip-rate for 3 My are shown in black. Note that the Fucino fault bounds an internally drained basin, which contained a large lake until it was drained for agriculture in 1874. Roman numerals correspond to the rivers introduced in Fig. 2 and Section 3.

Figure 2 Long profiles of selected rivers **(a)** crossing normal faults that increased their slip rate at ~0.8 Ma and are still undergoing a transient response to this tectonic perturbation, and **(b)** crossing normal faults that have moved at a constant slip-rate for 3 My. Roman numerals correspond to localities in Fig. 1 and channel descriptions in Section 3.

Figure 3 Catchments undergoing a transient response to tectonics, as defined by *Whittaker et al.*, 2007b: **(a)** Rio Torto **(b)** Torrente L'Apa, **(c)** Gole di Celano, **(d)** Rio di Aielli, **(e)** La Canala. Panel on the left shows hill-shade image from a 20m DEM for each catchment; the white dashed line delimits the zone of incision upstream of the active fault, which corresponds to the long profile convexities shown in Fig. 3. Green circles represent landslides with a volume greater than ~100 m^3, as mapped in the field. Panel on the right displays catchment boundary and trunk stream; the grey zone shows the area of the incised reach upstream of the fault; the contours represent the depth of incision derived from ArcMap, as measured from the elevation of the break in slope in the long profile. This is a proxy for the amount of incision since the increase in fault uplift rate occurred at ~0.8 Ma. Numbers in (a) show position of sampling sites for landslides/scree cones presented in Fig. 9a.

Figure 4 Fluvial sediment grain size, derived from Wolman point counts, against downstream distance for rivers crossing faults which have increased their slip rate. **(a)**

La Canala, crossing the Pescasseroli fault, **(b)** Torrente L'Apa, crossing the Fiamignano fault, **(c)** Rio Torto, crossing the Fiamignano fault, **(d)** Rio di Aielli, crossing the Fucino fault, and **(e)** Gole di Celano, crossing the Fucino fault. Black squares represent D_{84} values, open diamonds represent D_{50} values. The grey boxes correspond to the location of gorges upstream of the active faults, co-incident with the long profile convexities shown in Fig. 2. (a) to (e) are arranged in terms of increasing throw rate enhancement (arrow). Note changes in scale on both x and y-axis.

Figure 5 Fluvial sediment grain-size, derived from in situ sieving and weighing of sediment samples, against downstream distance for **(a)** Rio Torto, crossing the Fiamignano fault and **(b)** Gole di Celano, crossing he Fucino fault. Black circles represent D_{84} values, open circles represent D_{50} values. The grey boxes correspond to the location of gorges upstream of the active faults, co-incident with the long profile convexities shown in Fig. 2.

Figure 6 Fluvial sediment grain size, derived from Wolman point counts, against downstream distance normalised to the position of the active fault, for rivers crossing faults which have moved at a constant rate since 3 My, and have reached topographic steady-state with respect to on going fault uplift. Triangles represent the Fosso Tascino, crossing the Leonessa fault, and circles represent the Valleluce River, crossing the South Cassino fault. Black symbols represent D_{84} and open symbols represent D_{50}. The Leonessa and S. Cassino faults lie respectively at 12.5 and 9 km downstream of the source of their corresponding rivers.

Figure 7 (a) Maximum documented D_{84} upstream of the active faults, against the increase in slip rate the fault has undergone since 1 Ma. For catchments undergoing a transient response to tectonics, this maximum D_{84} corresponds to the peak in coarse fraction grain-size within the incised gorge marked by the grey box in Fig. 4; for steady-state catchments, it corresponds to the maximum D_{84} measured at any point upstream of the fault. **(b)** Average D_{84}, in the 2 km upstream of the active fault, as function of the slip rate increase.

Figure 8. Cumulative frequency distribution of the weighted fluvial sediment grain-size data for **(a)** the Rio Torto, crossing the Fiamignano fault, and **(b)** the Gole di Celano, crossing the Fucino fault. Results are presented in terms of downstream

distance, L, relative to the position of the fault, L_f. By definition the fault is at L/L_f = 1; "headwaters" refers to samples taken from the relatively unincised upper catchment, "gorge" refers to samples taken in the incised zone upstream of the fault, and "hangingwall" refers to samples downstream of the fault. The grey bars show derivation of D_{50} and D_{84} for these data, as presented in Fig. 5.

Figure 9 (a) Cumulative frequency distribution of grain-size for a selection of landslides (dotted lines) and scree cones (black lines) that directly enter the Rio Torto. Typical grain-size distribution of sediment in the upper part (i.e. not perturbed by tectonics) of both the Rio Torto and Celano catchments are shown for comparison. Numerals refer to the downstream position of these sampling sites, as shown on Fig. 3a. (**b**) Photo showing scree cones along the Rio Torto near sample site 3.

Figure 10 (a) Map of the of the Fucino area, showing the Fucino fault, the extent of the old lake, the two study rivers. The grey line shows the position of the cross section in (b), which is adapted from Cavinato *et al.*, 2002, and Whittaker *et al.*, 2008. Grey and black circles show upper Pleistocene grain-size sites presented in (c) for the Aielli and Celano fans respectively. **(b)** Cross section along line X – X' in (a) showing the hanging-wall stratigraphy. The "time" bar shows the age of the depositional sequences as identified by Cavinato *et al.* while the "stratigraphy" bar shows these in terms of sediment thickness. Only 100 m of upper Pleistocene lake sediments has been deposited above an identified tephra layer in the last 0.5 Ma, showing that the basin is substantially underfilled given the high rate of accommodation generation. In contrast, the slow sedimentation rate (0.2 mm/y) was approximately balanced the slow rate of accommodation generation in the late Pliocene and Early Pliocene. **(c)** Sediment grain-size distribution for upper Pleistocene fan deposits (grey and black circles in (a)), for Celano (dotted line) and Aielli (solid black line). Grey dashed lines show grain-size distribution for gravels interbedded with lake sediments near the villages of Aielli Stazione and Cerchio.

Figure 11. Synthesis diagram showing the erosional and depositional patterns characterizing the transient response of footwall catchments and hanging-wall basins to an increase in fault uplift rate as evidenced from the Central Apennines of Italy.

Table 1

River	*Fault*	*Downstream distance (km)* [a]	*Drainage area (km^2)* [a]	*initial slip rate (mm/y)* [b]	*Current slip rate (mm/y)* [b]	*% catchment incised*	*Incised volume (km^3)* [c]
Rio Torto	Fiamignano	10.5	62	0.3-0.35	1	20	0.9-1.6
Torrente L'Ape	Fiamignano	9.0	25	<0.1	0.25	10	0.2
Gole di Celano	Fucino	11.5 (from lake)	41	0.3-0.35	1.8	30	2-2.8
Rio di Aielli	Fucino	12.4 (to first fault)	38	0.3-0.35	1.8	40	2.6-3.5
La Canala	Pescasseroli	6.1	18	0.3-0.35	0.5	5	0.05
Fosso Tascino	Leonessa	12.7	45	0.3-0.35	0.35	n/a	n/a
Valleluce River	S. Cassino	9.3	20	0.3-0.35	0.3	n/a	n/a

[a]Measured at the fault

[b]Taken from Roberts and Michetti (2004) and Whittaker et al., (2007b)

[c]Upper bound calculated using geometrical correction as described in text

Figure 1

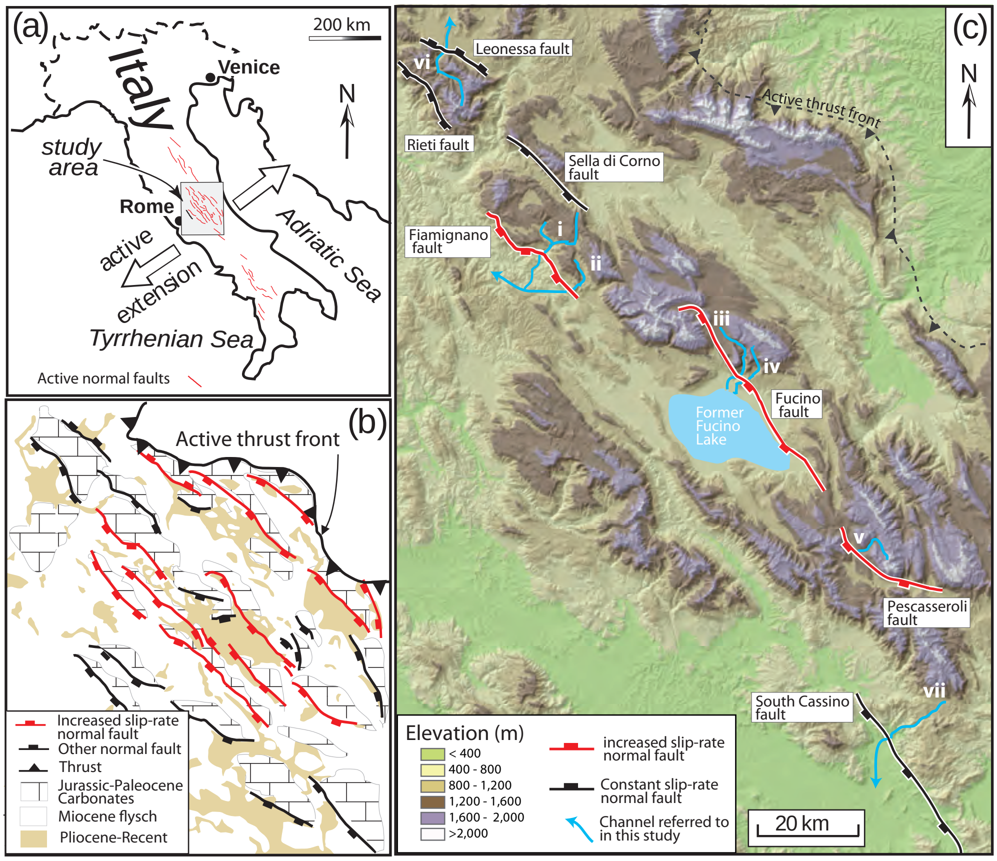
(a)
200 km
Italy
Venice
N
study area
Rome
active extension
Adriatic Sea
Tyrrhenian Sea
Active normal faults
(b)
Active thrust front
Increased slip-rate normal fault
Other normal fault
Thrust
Jurassic-Paleocene Carbonates
Miocene flysch
Pliocene-Recent
(c)
N
Leonessa fault
vi
Rieti fault
Sella di Corno fault
Active thrust front
Fiamignano fault
i
ii
iii
iv
Fucino fault
Former Fucino Lake
v
Pescasseroli fault
South Cassino fault
vii
Elevation (m)
< 400
400 - 800
800 - 1,200
1,200 - 1,600
1,600 - 2,000
>2,000
increased slip-rate normal fault
Constant slip-rate normal fault
Channel referred to in this study
20 km

Fig. 2

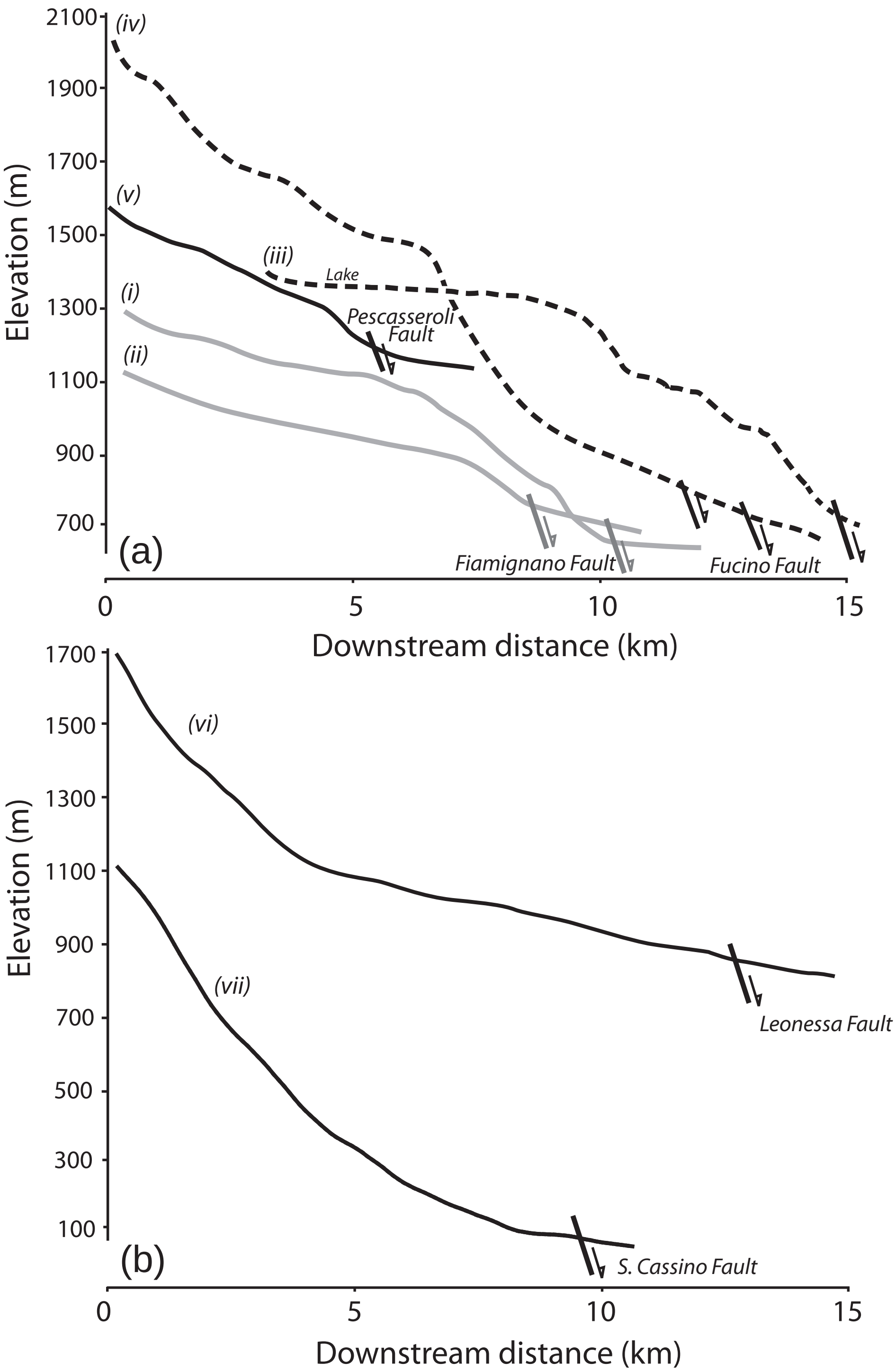

(a)
Elevation (m)
2100
1900
1700
1500
1300
1100
900
700
(iv)
(v)
(iii)
Lake
(i)
(ii)
Pescasseroli Fault
Fiamignano Fault
Fucino Fault
0
5
10
15
Downstream distance (km)
(b)
Elevation (m)
1700
1500
1300
1100
900
700
500
300
100
(vi)
(vii)
Leonessa Fault
S. Cassino Fault
0
5
10
15
Downstream distance (km)

Figure 3

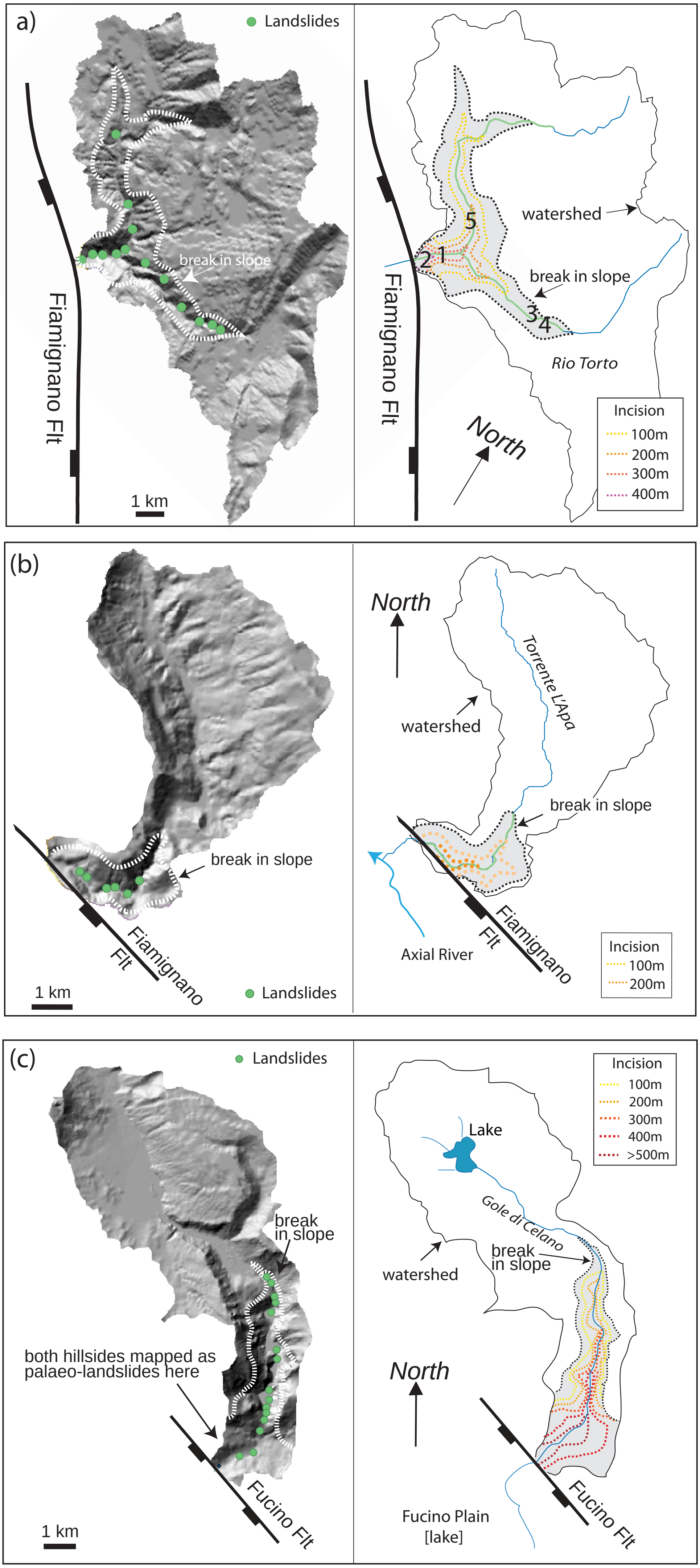

a)
Landslides
break in slope
Fiamignano Flt
1 km
watershed
5
2
1
break in slope
3
4
Rio Torto
Fiamignano Flt
North
Incision
100m
200m
300m
400m
(b)
break in slope
Fiamignano
Flt
1 km
Landslides
North
Torrente L'Apa
watershed
break in slope
Axial River
Fiamignano
Flt
Incision
100m
200m
(c)
Landslides
break
in slope
both hillsides mapped as
palaeo-landslides here
Fucino Flt
1 km
Incision
100m
200m
300m
400m
>500m
Lake
Gole di Celano
break
in slope
watershed
North
Fucino Plain
[lake]
Fucino Flt

Figure 3

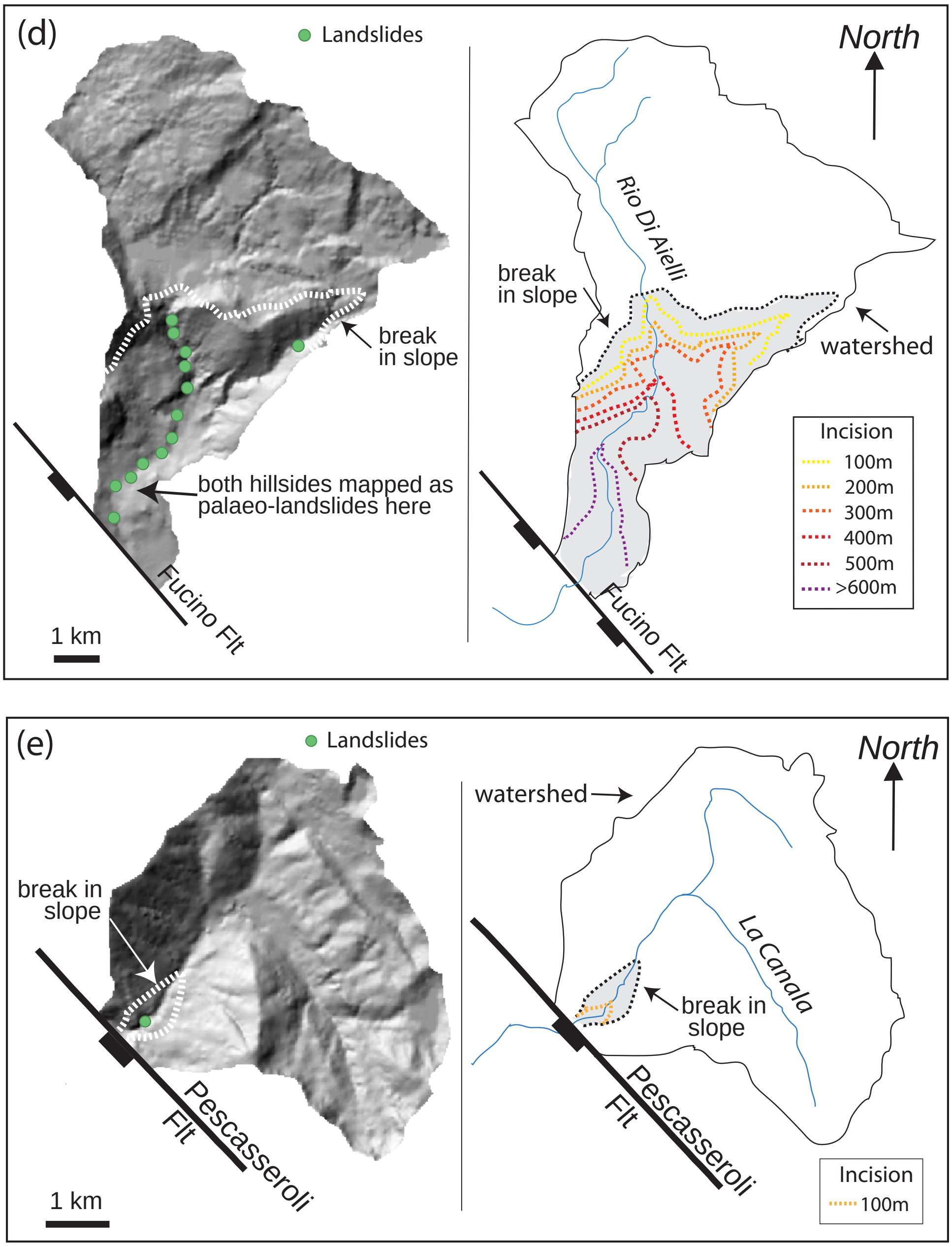

(d)
Landslides
North
break
in slope
both hillsides mapped as
palaeo-landslides here
Fucino Flt
1 km
Rio Di Aielli
break
in slope
watershed
Incision
100m
200m
300m
400m
500m
>600m
Fucino Flt
(e)
Landslides
North
break in
slope
Pescasseroli
Flt
1 km
watershed
La Canala
break in
slope
Pescasseroli
Flt
Incision
100m

Figure 4

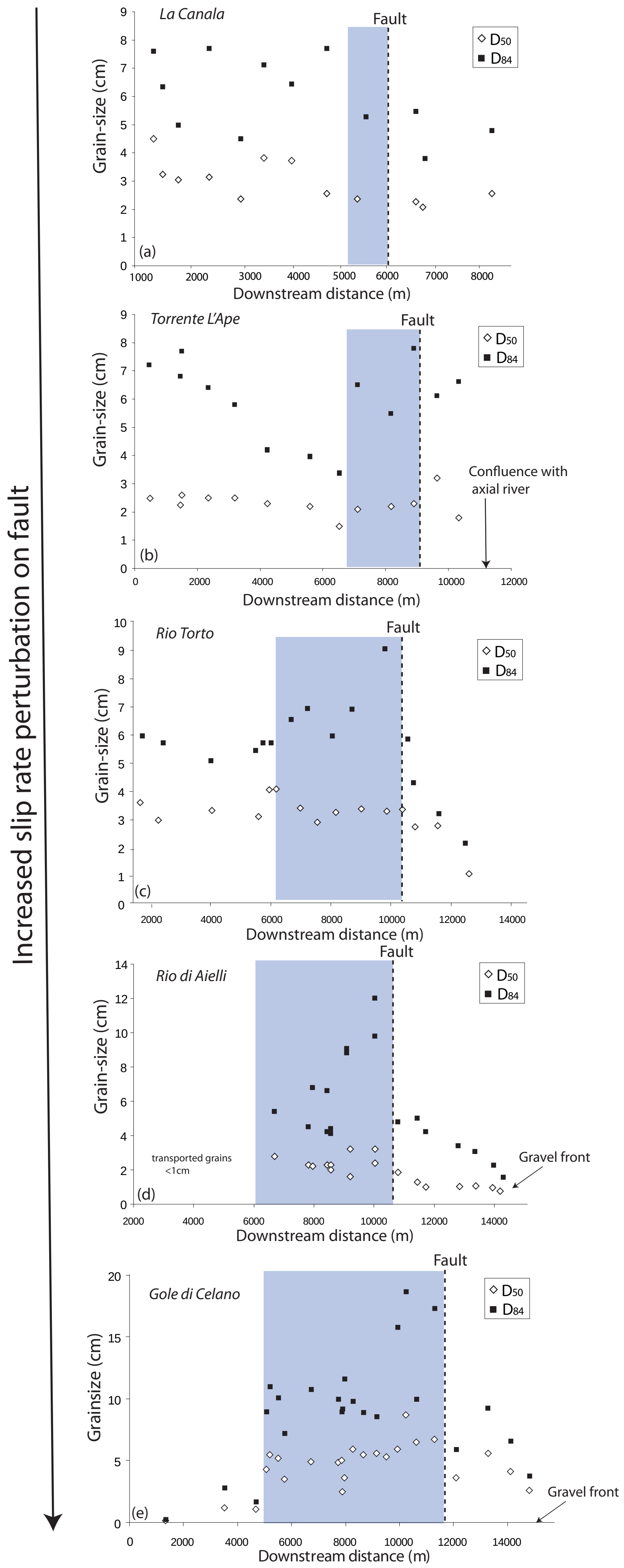

Increased slip rate perturbation on fault
La Canala
Fault
D50
D84
Grain-size (cm)
(a)
Downstream distance (m)
Torrente L'Ape
Fault
D50
D84
Confluence with axial river
Grain-size (cm)
(b)
Downstream distance (m)
Rio Torto
Fault
D50
D84
Grain-size (cm)
(c)
Downstream distance (m)
Rio di Aielli
Fault
D50
D84
transported grains <1cm
Gravel front
Grain-size (cm)
(d)
Downstream distance (m)
Gole di Celano
Fault
D50
D84
Gravel front
Grainsize (cm)
(e)
Downstream distance (m)

Figure 5

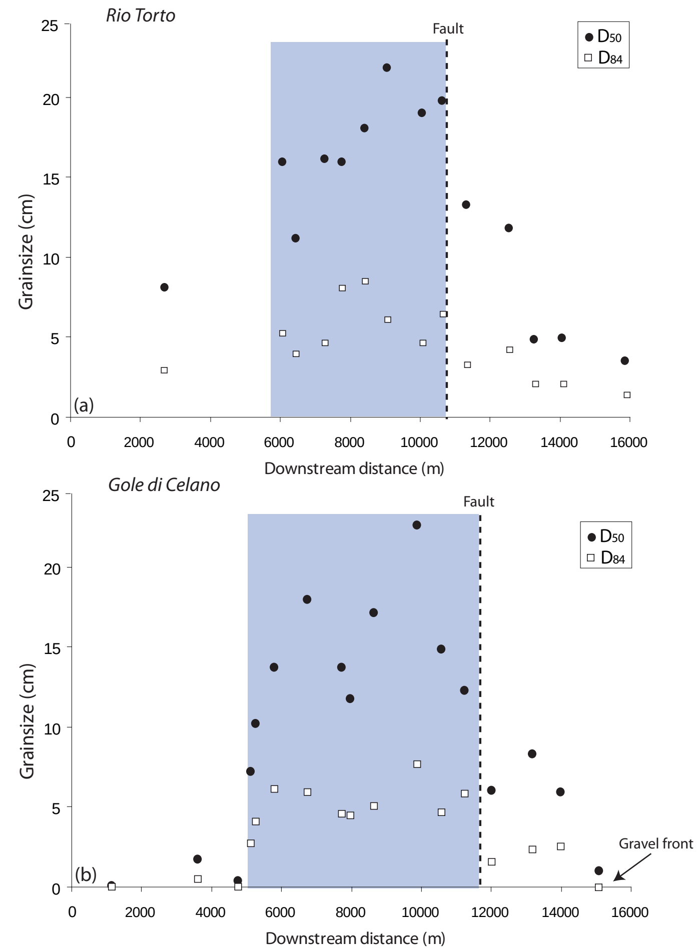
Rio Torto
Fault
D50
D84
Grainsize (cm)
(a)
Downstream distance (m)
Gole di Celano
Fault
D50
D84
Grainsize (cm)
Gravel front
(b)
Downstream distance (m)

Figure 6

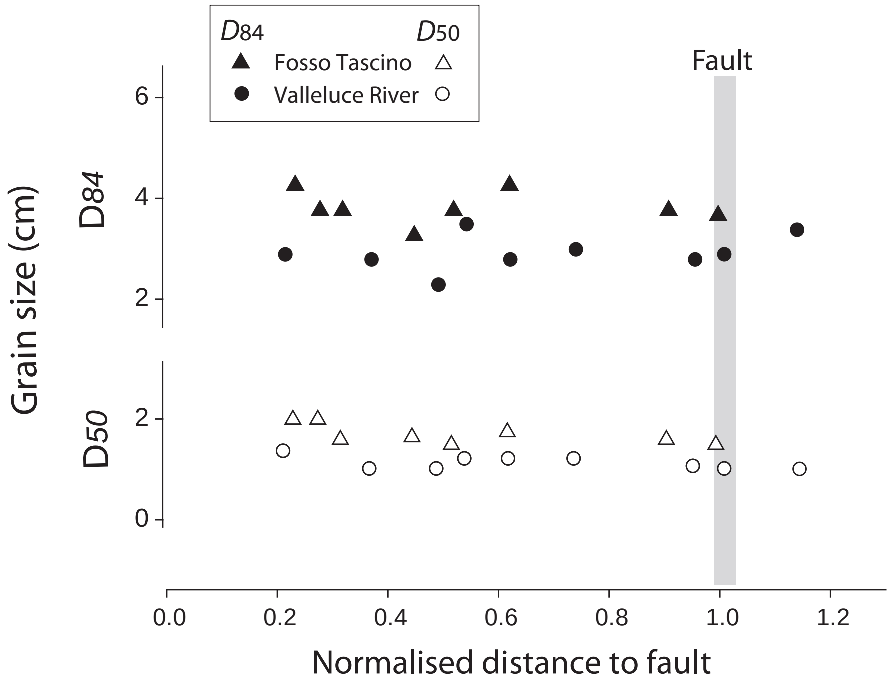

D84
D50
Fosso Tascino
Valleluce River
Fault
Grain size (cm)
D84
D50
6
4
2
2
0
0.0
0.2
0.4
0.6
0.8
1.0
1.2
Normalised distance to fault

Figure 7

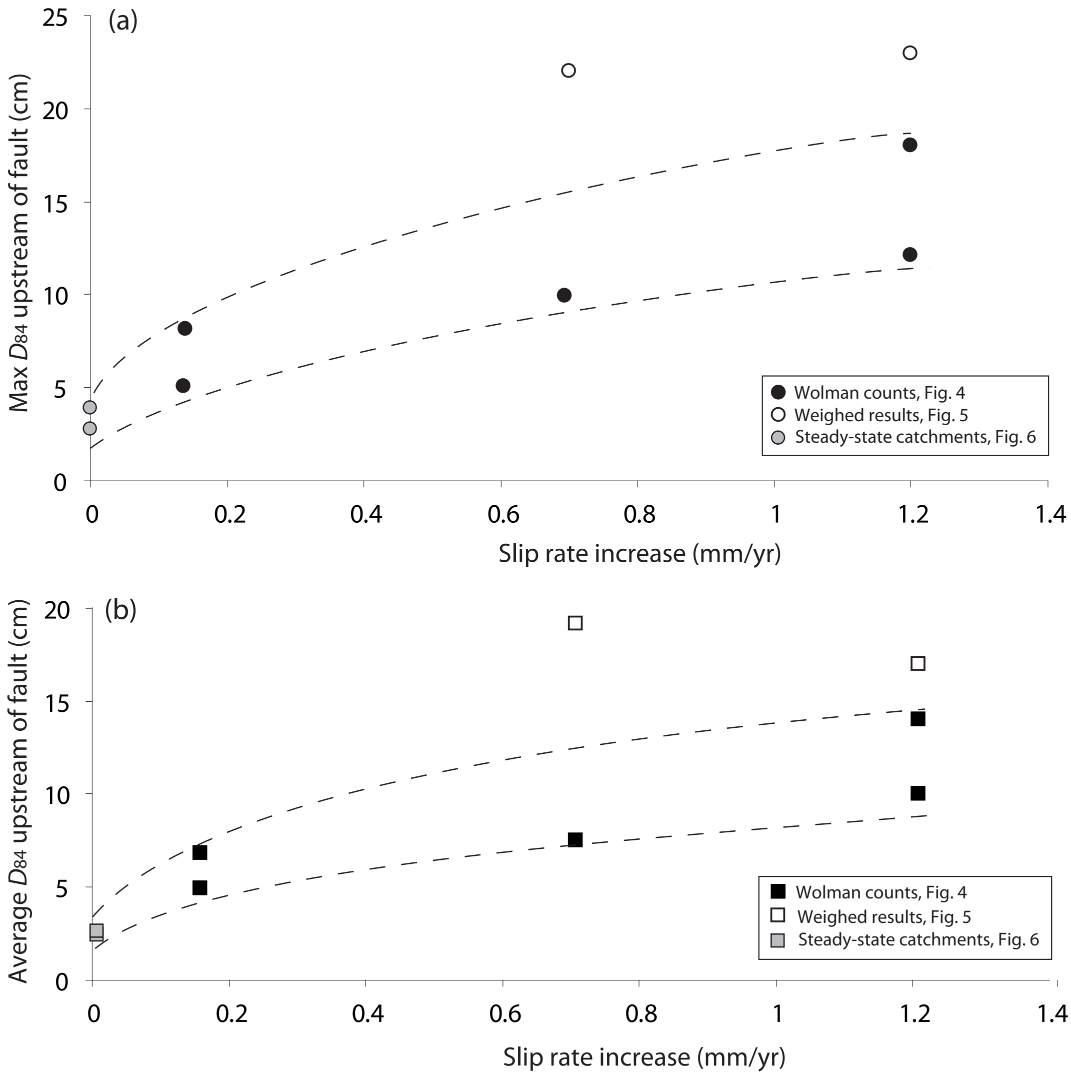

(a)
Max D_{84} upstream of fault (cm)
25
20
15
10
5
0
0
0.2
0.4
0.6
0.8
1
1.2
1.4
Slip rate increase (mm/yr)
Wolman counts, Fig. 4
Weighed results, Fig. 5
Steady-state catchments, Fig. 6
(b)
Average D_{84} upstream of fault (cm)
20
15
10
5
0
0
0.2
0.4
0.6
0.8
1
1.2
1.4
Slip rate increase (mm/yr)
Wolman counts, Fig. 4
Weighed results, Fig. 5
Steady-state catchments, Fig. 6

Figure 8

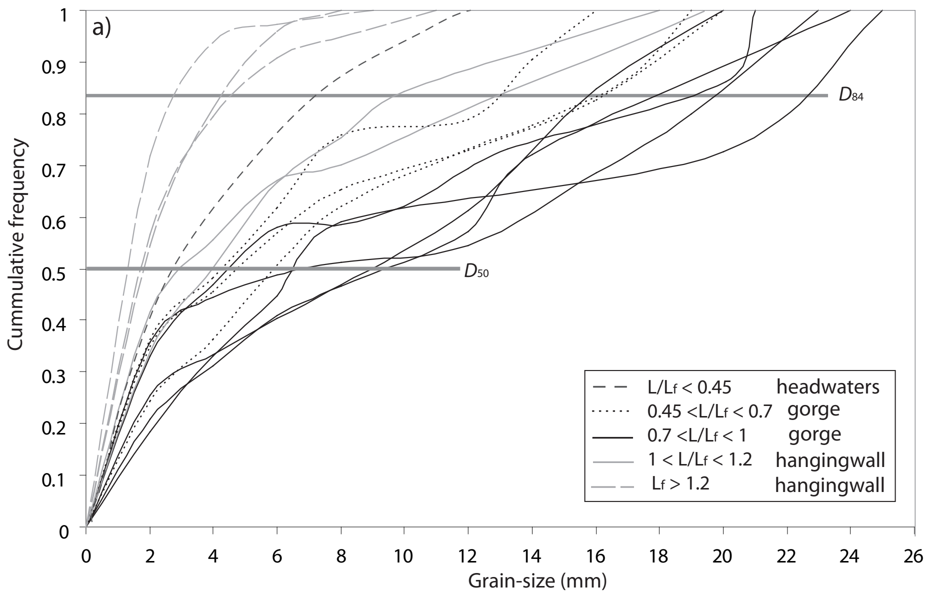

a)
Cummulative frequency
Grain-size (mm)
D84
D50
L/Lf < 0.45 headwaters
0.45 <L/Lf < 0.7 gorge
0.7 <L/Lf < 1 gorge
1 < L/Lf < 1.2 hangingwall
Lf > 1.2 hangingwall

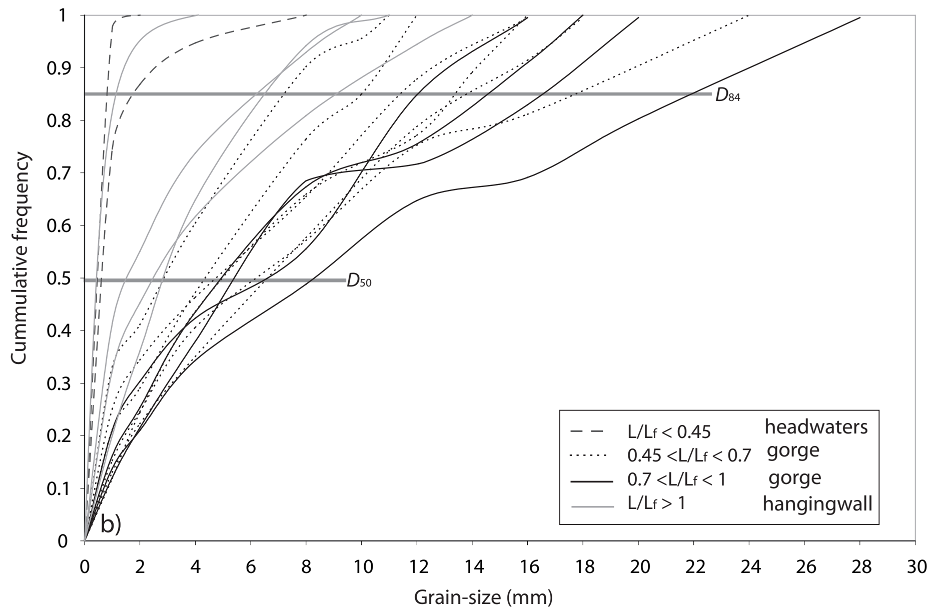

b)
Cummulative frequency
Grain-size (mm)
D84
D50
L/Lf < 0.45 headwaters
0.45 <L/Lf < 0.7 gorge
0.7 <L/Lf < 1 gorge
L/Lf > 1 hangingwall

Figure 9

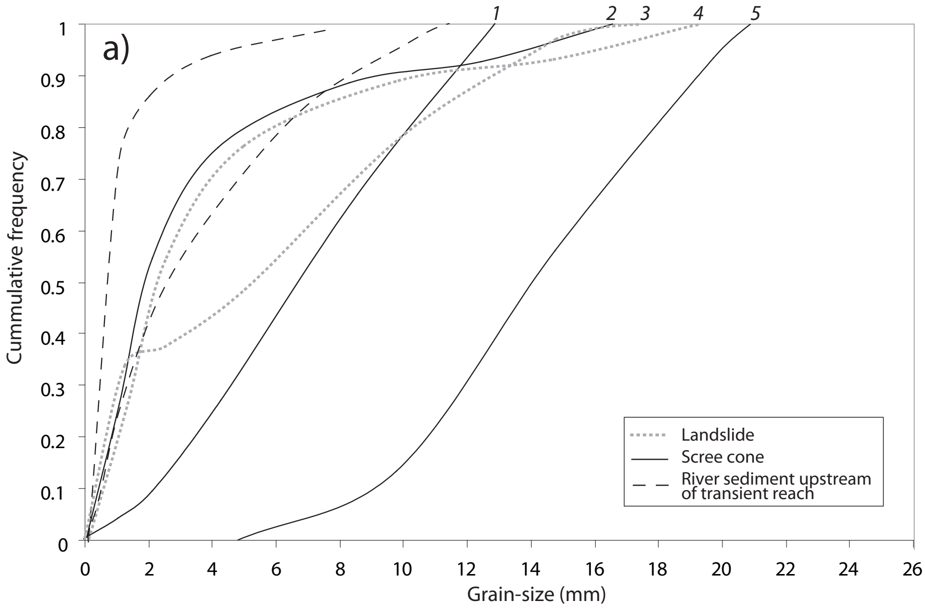
a)
1
2
3
4
5
Cummulative frequency
Grain-size (mm)
0
0.1
0.2
0.3
0.4
0.5
0.6
0.7
0.8
0.9
1
0
2
4
6
8
10
12
14
16
18
20
22
24
26
Landslide
Scree cone
River sediment upstream of transient reach

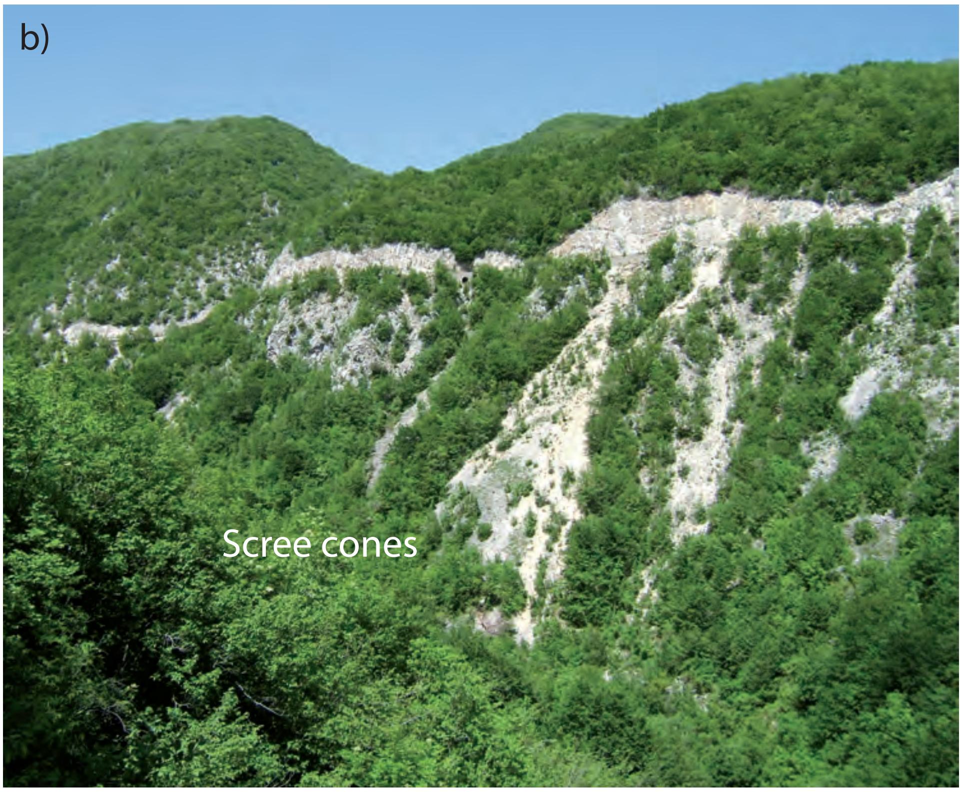
b)
Scree cones

Figure 10

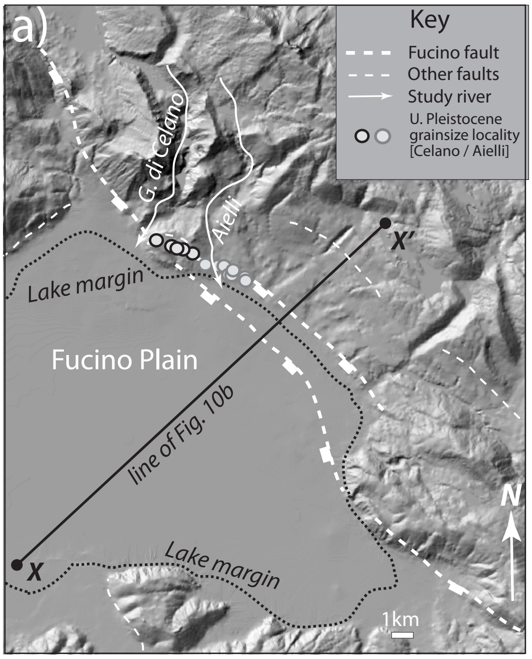
a)
Key
Fucino fault
Other faults
Study river
U. Pleistocene grainsize locality [Celano / Aielli]
G. di Celano
Aielli
X′
Lake margin
Fucino Plain
line of Fig. 10b
N
X
Lake margin
1km

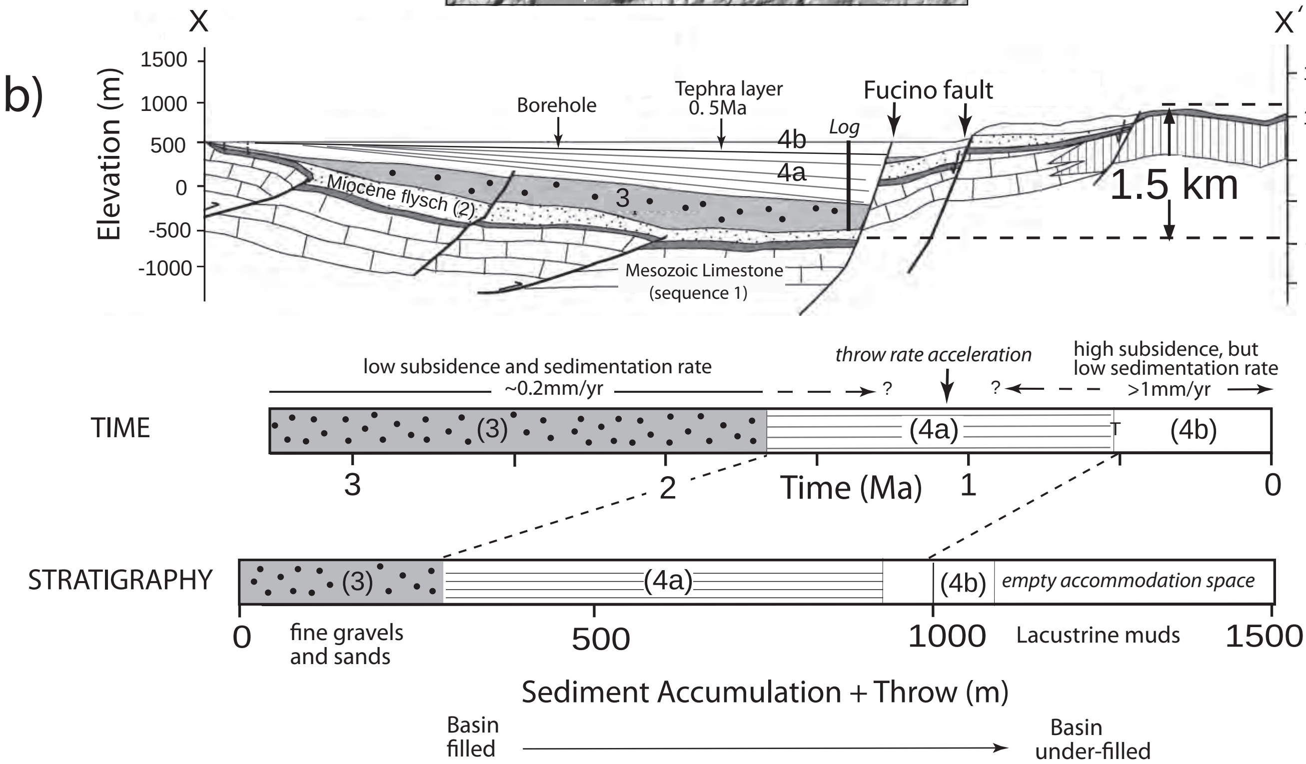
X
X′
b)
Elevation (m)
1500
1000
500
0
-500
-1000
Borehole
Tephra layer
0. 5Ma
Fucino fault
Log
4b
4a
3
Miocene flysch (2)
Mesozoic Limestone
(sequence 1)
1.5 km
low subsidence and sedimentation rate
~0.2mm/yr
throw rate acceleration
high subsidence, but low sedimentation rate
>1mm/yr
TIME
(3)
(4a)
(4b)
3
2
Time (Ma)
1
0
STRATIGRAPHY
(3)
(4a)
(4b)
empty accommodation space
0
fine gravels and sands
500
1000
Lacustrine muds
1500
Sediment Accumulation + Throw (m)
Basin filled
Basin under-filled

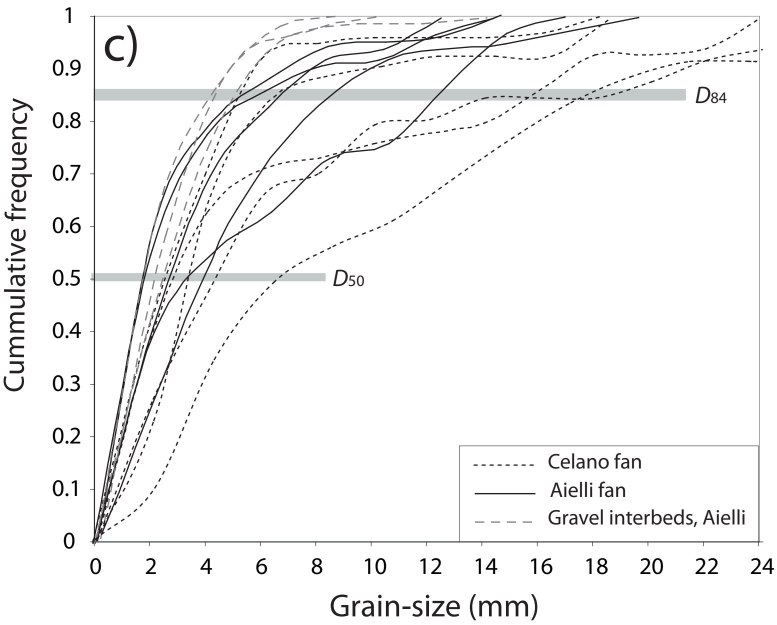
c)
Cummulative frequency
D84
D50
Celano fan
Aielli fan
Gravel interbeds, Aielli
Grain-size (mm)
0
2
4
6
8
10
12
14
16
18
20
22
24
0.1
0.2
0.3
0.4
0.5
0.6
0.7
0.8
0.9
1

Figure 11

Transient sedimentological response to tectonic perturbation